

Using Inertial Measurement Units originally developed for biomechanics for modal testing of civil engineering structures

David Hester^a, James Brownjohn^b, Mateusz Bocian^c, Yan Xu^b, Antonino Quattrone^d

^aSchool of Natural and Built Environment, Queen's University Belfast, UK

^bVibration Engineering Section, University of Exeter, UK

^cDepartment of Engineering, University of Leicester, UK

^dCivil and Construction Engineering, Politecnico di Torino, Italy

Abstract

This paper explores the use of wireless Inertial Measurement Units (IMU) originally developed for bio-mechanical research applications for modal testing of civil engineering infrastructure. Due to their biomechanics origin, these devices combine a triaxial accelerometer with gyroscopes and magnetometers for orientation, as well as on board data logging capability and wireless communication for optional data streaming and to coordinate synchronisation with other IMUs in a network. The motivation for application to civil structures is that their capabilities and simple operating procedures make them suitable for modal testing of many types of civil infrastructure of limited dimension including footbridges and floors while also enabling recovering of dynamic forces generated and applied to structures by moving humans. To explore their capabilities in civil applications, the IMUs are evaluated through modal tests on three different structures with increasing challenge of spatial and environmental complexity. These are, a full-scale floor mock-up in a laboratory, a short span road bridge and a seven story office tower. For each case, the results from the IMUs are compared with those from a conventional wired system to identify the limitations. The main conclusion is that the relatively high noise floor and limited communication range will not be a serious limitation in the great majority of typical civil modal test applications where convenient operation is a significant advantage over conventional wired systems.

Keywords: Operational Modal analysis; Wireless sensors; Ambient vibration; Civil engineering structures.

1.0 Introduction

The conventional view of civil infrastructure health monitoring is an array of permanently installed instrumentation with continuous data acquisition and data interpretation. Such structural health monitoring (SHM) systems are usually deployed on new landmark structures, with practically every new long suspended span bridge design including permanent instrumentation. There is an argument that such large structures will not benefit from SHM until they begin to age and that resources would be more effectively deployed on a larger number of smaller, older, but still critical infrastructure components such as the many masonry arch bridges and viaducts built in Victorian Britain. The large number of these older structures (e.g. tens of thousands of bridges in the UK) rule out comprehensive permanent monitoring, but there is a case for peripatetic monitoring systems for vibration and load testing. Such relocatable instrumentation arrays must be deployable easily and rapidly.

40 Short term instrumentation typically comprises strain gauges and/or accelerometers [1]. Strain
41 gauges are primarily used for capturing static and quasi-static effects with accelerometers primarily
42 capturing dynamic effects. In fact accelerometers are widely used for structural identification (St-id),
43 which comprises system identification (modal analysis) designed to validate numerical models and
44 to understand and predict dynamic performance [2]. Accelerometers deployed in civil infrastructure
45 St-id applications have traditionally been large wired devices using piezo-electric sensing elements
46 or servo-control of a proof mass. Requirements from a wide range of user communities have driven
47 development of micro electrical mechanical system (MEMS) accelerometers that are small, light,
48 inexpensive and low power. The potential to deploy MEMS accelerometers for civil infrastructure
49 SHM applications has led to a large volume of research in smart wireless accelerometers for long-
50 term deployment. Most such sensors have been designed and deployed by the research community,
51 with exemplar applications such as the large scale Imote2 deployment on Jindo Bridge [3]. While
52 most SHM research has gone on long term deployments of wireless sensors, few deployments focus
53 on short term investigations [4]. Also, while there are many commercial solutions for wireless
54 sensing of non-dynamic data there are fewer commercial wireless accelerometers. These are
55 generally optimised applications such as in automotive and aerospace engineering where
56 acceleration ranges are relatively large compared to the sub-1 g ranges experienced in operational
57 monitoring of civil infrastructure such as bridges and buildings.

58

59 Accelerometers have been used in the biomechanics community for many years e.g. for gait analysis
60 [5]. Inertial measurement units (IMUs) were developed with incorporation of gyroscopes [6] and
61 magnetometers, and were subsequently available for wireless data acquisition [7]. Demand from the
62 biomechanics community with applications in health and sport have driven development of
63 commercial systems that are used in short term in-vivo instrumentation e.g. for hospital outpatient
64 diagnosis, movement science experiments and for study and enhancement of sports performance.
65 These systems both complement and replace optics-based motion capture systems and may be used
66 with force plates and instrumented treadmills. The large rotations and translations involved require
67 conversion to global (world) coordinate systems (WCS) but other than this, the requirements for
68 size, weight, wireless communication and low power are remarkably similar to the requirements for
69 vibration measurements of civil infrastructure. This was the experience of the authors when using
70 biomechanics IMUs for tracking human movements in open space as part of research on vibration
71 serviceability of footbridges [8].

72 Problematic footbridge vibrations occur at frequencies (0.5 Hz to 5 Hz) consistent with the frequency
73 range of biomechanics applications, the vibration levels are well above their resolution levels and
74 noise floors, and their spans do not usually exceed the range limits for wireless transmission.
75 The typical civil field applications are time-constrained, logistically demanding and with restricted
76 access for cabling. Hence a system that is readily transported, can be deployed rapidly and does not
77 need cables is a very attractive proposition. The research described here aimed to find out if the
78 limited resolution would be a show stopper for application in less lively structures such as tall
79 buildings and road bridges.

80 This paper begins by describing how wired and wireless sensors are traditionally used for vibration
81 testing, noting their strengths and limitations. A detailed comparison of performance IMUs with a
82 wired system is described for the floor mockup, followed by description of applications to a short
83 span highway bridge and a nine-storey university building.

84 1.1. Wired accelerometer systems in modal testing of civil infrastructure

85 While only a single accelerometer is needed to estimate modal frequencies and damping ratios, full
86 description of modal properties additionally requires estimation of mode shapes and modal masses,
87 two properties frequently combined in the form of scaled mode shapes. Estimation of the full set of
88 modal properties such as in ground vibration testing of aircraft [9] and vibration serviceability
89 evaluation of lively floors in offices and hospitals [10] requires measurement of excitation force
90 usually due to one or more shakers and acceleration response at multiple locations in a modal test
91 [11]. Various techniques of experimental modal analysis (EMA) are applied to recover the modal
92 properties and these require the force and response signals to be synchronised, since the
93 identification processes rely on phase relationships between and among force and response signals.

94 Where a force signal cannot be provided or cannot be measured, output only or ambient vibration
95 testing is used, and a range of techniques of operational modal analysis (OMA) are applied to
96 recover all modal properties with the exception of modal mass or mode shape scaling. Typical
97 applications of OMA include long span bridges [12], towers, chimneys [13] and tall buildings and
98 other structures[14]. The requirements of synchronous measurement of all response signals also
99 apply.

100 Wired systems have varied architecture, with a large range of multichannel acquisition and analysis
101 systems to choose from. The front end of such systems is nowadays typically a simultaneous sample
102 and hold buffer to capture all signals at the same time instant, feeding a 24 bit analog digital
103 converter which means that little or no signal amplification is required due to having bit-level
104 precision below the sensor noise floor. With wired systems, choice of accelerometer and
105 corresponding power supply signal conditioning allows for optimisation to application using high
106 resolution sensors such as the PCB piezo-electric [15], Honeywell Quartz-Flex [16] or Kinematics
107 servo- accelerometers [17]. An alternative to comprehensive signal analysis systems, bespoke
108 systems built from multi-channel acquisition front ends in a component system (e.g. National
109 Instruments) allow for flexible architecture providing signals for processing using separate modal
110 analysis software.

111 1.2 Wireless sensing for civil engineering structures

112 The past two decades have seen significant effort on developing wireless sensing systems for civil
113 engineering structures, especially bridges. This effort has been largely motivated by the logistical
114 difficulties experienced when installing wired systems, however developments have been targeted
115 at permanent monitoring systems rather than temporary systems. Hence wireless accelerometers
116 developed and adapted by civil engineering researchers [18-20] have been optimised for low power
117 operation with efficient real time data transmission and on board processing to reduce power
118 requirements and the need for downstream data reduction. The ultimate wireless accelerometer
119 demonstration is the Jindo Bridge project [21]. There are few applications of such wireless
120 accelerometers for short term measurement campaigns such as modal testing [22,23] because their
121 optimisation for long term monitoring and on-board processing means they are not well suited for
122 the demands of a modal testing campaign.

123 While modal testing requires synchronous data acquisition, this does not necessarily mean that data
124 must be transmitted to a base station for analysis in real time. Hence a system of autonomous

125 recorders conventionally deployed in seismic monitoring, and with GPS synchronisation can be used
126 for distributed data acquisition with data from separate units merged in post processing for modal
127 analysis. Systems from Guralp and GeoSIG provide this capability and the latter was deployed for
128 ambient vibration testing of Humber Bridge in 2008 [24]. In the absence of a GPS signal, precision
129 clocks can be used to synchronise recorders [25-27] but these are usually for high-end applications,
130 and there is justification for low-cost devices with limited capabilities and simple operation in certain
131 circumstance. The aim of this paper is to show the capabilities and limitations of such a system.

132 1.3 Objectives

133 Wireless sensor systems for Civil Engineering structures have been optimised for long term
134 monitoring and real time data transmission to a base station e.g. Imote2 [19]. For modal testing with
135 tight timing and logistical constraints the time spent establishing a wireless network for real time
136 transmission is not a good investment when reliable synchronous data collection is all that is
137 needed. It is capability and performance in this respect that is investigated in this paper, as modal
138 tests need to be time-efficient with easy to deploy accelerometers. Authors have found that a modal
139 test (of a footbridge) can be reduced to carrying a handful of IMUs to site in a coat pocket, resting
140 them on the bridge surface at selected measurement points for set duration then collecting the
141 IMUs and returning to base. Subsequent downloading and merging of data from each IMU is equally
142 simple. This paper explores the limits of capability of a particular type of IMU designed for
143 biomechanics applications when used for modal testing of a representative set of civil structures.

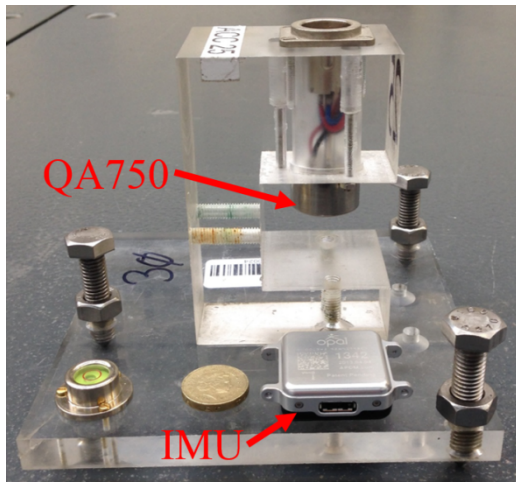
144 **Identifying capabilities and limitations will build confidence in using the IMUs for**
145 **modal testing of specific structures by comparison with high resolution wired**
146 **accelerometers, focusing on synchronisation and resolution. To begin, the IMUs**
147 **and wired (reference) sensors are described in section 2, then the ability of the**
148 **IMUs to capture the mode shapes is examined for three different structures: a**
149 **laboratory floor structure (5 m x 7.5 m), a steel road bridge (36 m span), and a 7**
150 **story concrete office building. These results are reported in sections 3, 4 and 5**
151 **respectively. It is shown that broadly speaking the frequencies and mode shapes**
152 **obtained from the IMUs agreed very well with those obtained from the wired**
153 **system. 2.0 Description of wired and wireless sensors used**

154 2.1 Wired accelerometers: Honeywell QA-750 force balance accelerometers

155 The reference accelerometers used here are Honeywell QA-750 quartz-flex force balance
156 accelerometers. These are inertial grade uniaxial accelerometers historically used for inertial
157 guidance (aerospace) and directional drilling (oil/gas industry). Their low noise floor and frequency
158 response to DC has allowed their successful use for many years for the modal testing of a range of
159 civil engineering structures. They are also used in the structural health monitoring systems installed
160 on Hong Kong's long span bridges [28]. These accelerometers comprise a sprung proof mass moving
161 in a magnetic coil whose current, generated by a servo-controller keeps the mass in position. For
162 field testing described in this paper the current signal is dropped across an external 1 k Ω resistor so
163 that effective scale factor is approximately 1.3 V/g and using a 24 bit analogue to digital converter
164 (ADC) with $\pm 5V$ range, bit level resolution is 0.155 μg (1.52 $\mu m.s^{-2}$). The accelerometer is mounted in
165 a perspex housing shown in Fig. 1. This may be attached to a structure using glue or magnets, but

166 more usually the housing is attached to a base plate with three levelling screws (Fig. 1) that rest on
167 the horizontal surface of a structure whose vibration levels are usually a small fraction of gravity. The
168 stiff mounting has no effect on the performance of the QA in the range of frequencies measured on
169 civil structures.

170



171

172 Fig. 1, Honeywell QA 750 accelerometer mounted in perspex housing with Opal IMU left on the base
173 plate.

174 2.2 Wireless accelerometers (IMUs)

175 The IMU used here is the APDM Opal™ shown in Fig. 1 placed on the perspex base plate of the QA-
176 750 accelerometer. For size reference, a £1 sterling coin is also shown in the figure.

177 IMUs were originally developed for clinical research in biomechanics [29] and the fusion of data
178 from three types of sensor promotes them to Attitude and Heading Reference Systems (AHRS). The
179 Opal is one type of AHRS described in [29]. The on board magnetometer, triaxial accelerometer and
180 triaxial gyroscope provide data on motion and orientation. Each Opal IMU also incorporates a
181 temperature gauge, flash memory, and communication managed by an on-board microcontroller. In
182 this study vertical and biaxial horizontal acceleration with respect to the local coordinate system of
183 the IMU are used and the gyro and magnetometer data are not needed to transform accelerations
184 to WCS. With the 14-bit ADC the ± 2 g and ± 6 g ranges offered correspond to bit-level resolution of
185 $240 \mu\text{g}$ (2.35 mm.s^{-2}) and $730 \mu\text{g}$ (7.19 mm.s^{-2}). For all the measurements described here the sample
186 rate was set to 128 Hz per channel.

187 Of great importance to the performance of any compound (e.g. multi-agent/unit) wireless
188 measurement system is the capability for synchronised data capture. Opal™ IMUs are synchronised
189 in one of two ways, either with or without a wireless access point allowing rapid data streaming to
190 the host computer. In the former mode, denoted as a synchronised streaming mode (SSM), any
191 deviations in the timing of data collected by IMUs are adjusted to the master time of the host
192 computer. Due to its dependence on access point connectivity, SSM is suitable for laboratory
193 environments of relatively small dimensions. In the latter mode, denoted as synchronised logging
194 mode (SLM), the timing of data capture is adjusted according to a probabilistic model, based on a

195 network of individual clocks of all units. The data are recorded onto the memory of each unit and
196 downloaded offline via a docking station. SLM is suitable for applications in which immediate data
197 accessibility is not of critical importance.

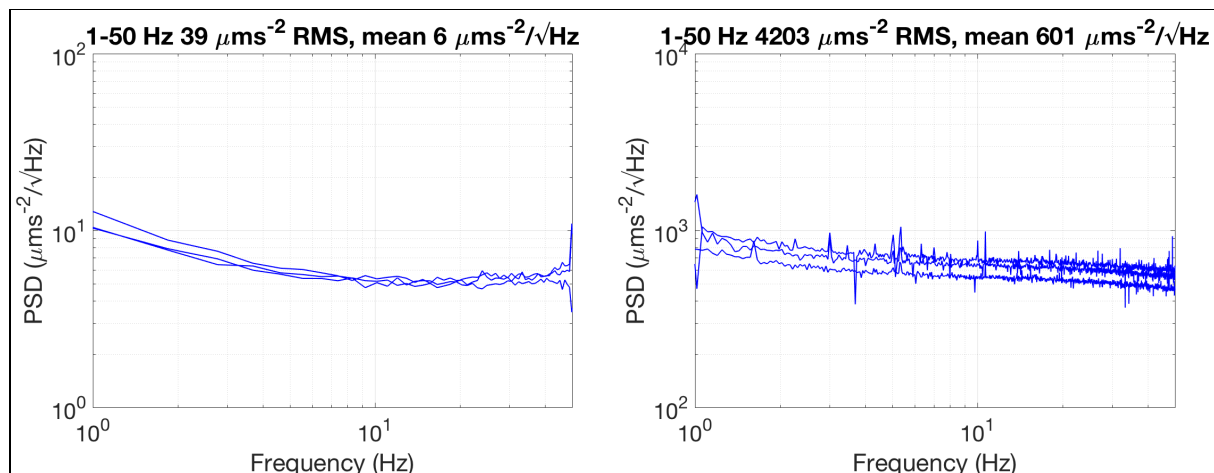
198 When operating in SSM the IMUs need to remain within 30 m of the wireless access point to
199 maintain synchronisation. Definite information on the maximum distance between IMUs allowing
200 synchronisation to be maintained when operating in SLM is not available. Essentially, having been
201 developed for applications in biomechanical research, situations where the IMU were tens of meters
202 apart were unlikely to occur. In this study the sensors will be used in SLM as the requirement to set
203 up a wireless access point on a civil engineering structure is logistically undesirable. In SLM if the
204 IMU's are out of range with each other they each keep time using their own internal clock. Once this
205 occurs, some drift is possible between individual sensors, with larger drifts likely if there are large
206 temperature ranges among sensors. Synchronisation drift is an important issue as it can affect modal
207 analysis procedures [30], but because wireless communication and synchronisation effects on modal
208 analysis are affected by a very wide range of factors it is not studied here. Instead the aim is to
209 examine if the potential errors identified above are sufficiently small that the mode shapes obtained
210 based on data from IMUs are still identified correctly.

211 As part of a previous study [31] it was shown that IMU's could be used to capture the mode shapes
212 of a relatively flexible cable supported footbridge. However, significant questions remained as to
213 how the IMUs would perform on more common civil engineering structures such as road bridges and
214 office towers, where the amplitudes of vibration will be significantly smaller than on a cable
215 supported footbridge and synchronisation between sensors could be affected by larger distances
216 and physical barriers such as walls/floors between the IMUs. These questions are addressed in this
217 current work.

218 2.3 Sensor noise floor

219 Manufacturer data for the two sensors quotes sensor noise floor for the QA-750 as $7 \mu\text{g}/\sqrt{\text{Hz}}$ in 0-10
220 Hz band and for the Opal™ as $128 \mu\text{g}/\sqrt{\text{Hz}}$. A test of the sensors in quiet laboratory conditions was
221 used to check these figures. In two separate exercises in different laboratories and times, signals
222 from three co-located sensors were acquired. Any coherent response due to small vibrations in the
223 quiet laboratory is filtered to leave non-coherent signals representing noise [32]. The result is shown
224 in Fig. 2. In both cases the self-noise is below the manufacturer specification and in fact the Opal
225 self-noise, for the sensor operating in the 6 g range, is below the bit-level resolution. The Opal noise
226 floor is 10 times greater than for the QA.

227 The effect of sensor noise floor on accuracy of modal identification is beyond the scope of this paper
228 although recent research [33] has been able to quantify the effect of (response) signal to (sensor)
229 noise ratio for Bayesian operational modal analysis. A pilot study [26] comparing IMUs and QA for
230 ambient response of a footbridge has shown that the effect of IMU noise floor on frequency and
231 damping estimation uncertainty in one specific application is insignificant.



232 Fig. 2, Power spectral density of sensor self-noise for QA-750 (left) and Opal IMU (right).

233 **3.0 Laboratory Trial**

234 The laboratory trial was split into two parts. Initially both sensors (QA and IMU) were placed on a
 235 shaker to see how the IMU performed relative to the QA across a range of amplitudes and
 236 frequencies (section 3.1). Subsequently data from both sensors were used to calculate the mode
 237 shapes of a steel floor structure that was built in the laboratory (section 3.2). Essentially Section 3.1
 238 checks the sensitivity/performance of the accelerometer in the IMU across the range of acceleration
 239 amplitudes and structural frequencies typically encountered on civil engineering structures and
 240 section 3.2 checks if under laboratory conditions the synchronisation between the different IMUs in
 241 the network is sufficiently accurate to allow mode shapes to be recovered accurately.

242 3.1 Performance of accelerometers when placed on shaker

243 Authors' experience of using the QA is that it is both accurate and reliable and hence very well suited
 244 to the demands modal testing of civil structures, but there are occasions when the full capability is
 245 not required and the expense not justified. Also technology developments lead to lower cost MEMS
 246 sensors that approach or even exceed the performance of QAs, which are regarded by authors as
 247 the standard against which all other accelerometers are judged.

248 Accelerometer calibration is provided by the manufacturers. For the QAs the calibration certificates
 249 state current output in mA/g which is converted to V/g using precision 1 kΩ load resistors, while for
 250 the IMUs the signals are converted to m.s⁻² by on board processor. In each case a simple check is
 251 obtained using the 1 g signal offset when measuring vertical acceleration. Using this methods, the
 252 set of five IMUs used in the experiment to generate Fig. 2 report gravity as 9.864 m.s⁻² with standard
 253 error 0.6% while the set of four QAs report gravity as 9.8305 with standard error 0.3%.

254 To examine how well the IMU performed with respect to the QA both sensors were mounted on a
 255 shaker (see Fig. 3) and a white noise excitation signal was provided to the shaker. The IMU was
 256 operating in SLM. The test lasted for approximately 10 minutes (600 seconds) and the time series
 257 recorded by both accelerometers (scanning rate 128 Hz) is shown in Fig. 4(a). The shaker was driven
 258 at a quarter of maximum force output to generate maximum accelerations in the region of ±1 m/s²
 259 which is the typical range of accelerations encountered on civil engineering structures. Fig. 4(b)
 260 shows a zoomed in view of one second of acceleration data and it can be seen that there is good

261 agreement between the signals from both accelerometers. The Welch method was used to calculate
 262 the frequency content of both signals in Fig. 4(a), with window length of 60 seconds, with no
 263 overlap, and the result is shown in Fig. 4(c). It can be seen in Fig. 4(c) and Fig. 4(d), which shows a
 264 zoomed in view between 4-5 Hz that the frequency content returned by both sensors is very similar.
 265 To further examine how closely the signal from the IMU matches the signal from the QA, the
 266 transfer function ($T_{qo}(f)$, Eq. 1) and magnitude squared coherence ($C_{qo}(f)$, Eq. 2) between the QA and
 267 the IMU are calculated and the results are plotted in Figs. 4(e) and (f) respectively.

$$268 \quad T_{QI}(f) = \frac{P_{IQ}(f)}{P_{QQ}(f)} \quad (1)$$

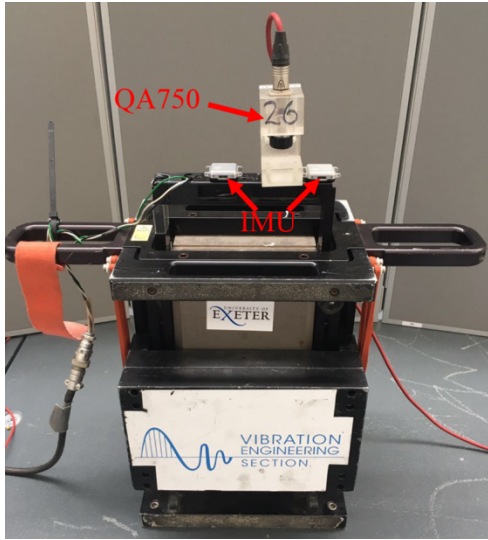
269

$$270 \quad C_{QI}(f) = \frac{|P_{IQ}(f)|}{P_{QQ}(f) P_{II}(f)} \quad (2)$$

271

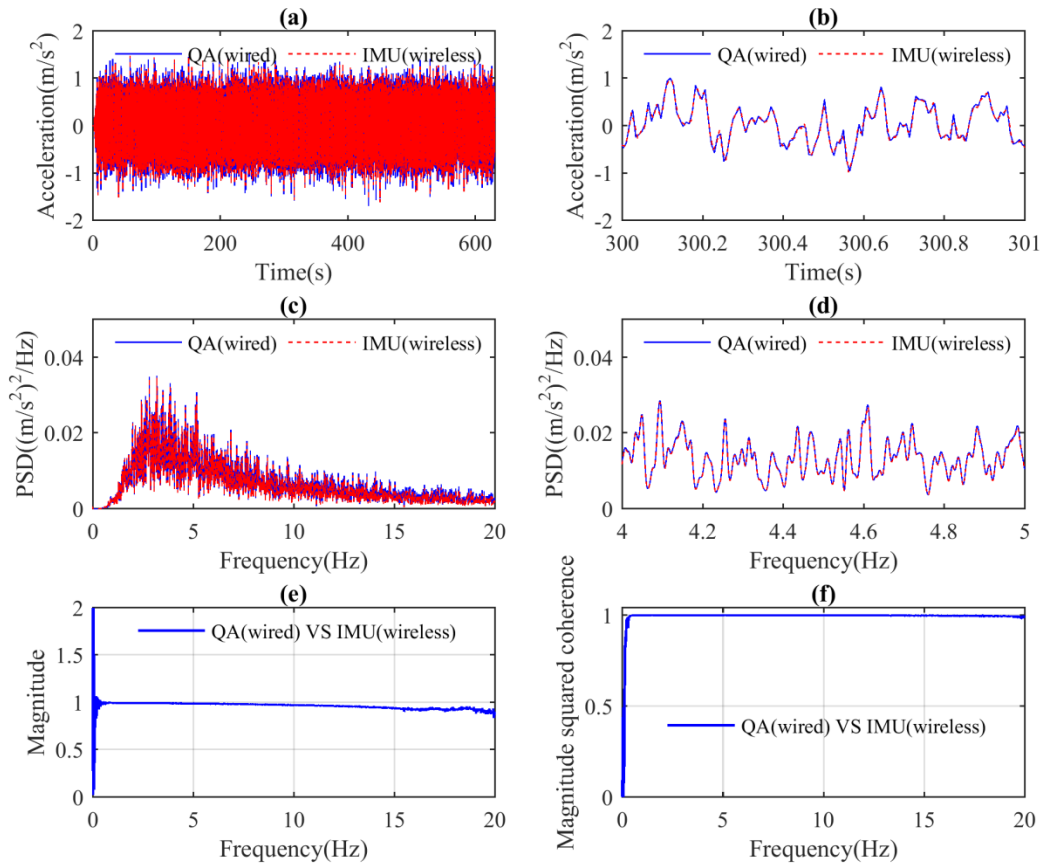
272 where P_{IQ} is the spectral density of the QA signal and the IMU signal, P_{QQ} is the power spectral
 273 density of the QA signal, and P_{II} is the power spectral density of the IMU signal. For both metrics
 274 ($T_{QI}(f)$ & $C_{QI}(f)$) values of close to one indicates a good match between the signals being analysed.
 275 Broadly speaking the plots in Figs. 4(e) and (f) remain close to one in the frequency range 0-20 Hz,
 276 with just the transfer function falling slightly below one for higher values of frequency. This indicates
 277 that for frequencies in the range 10-20 Hz the IMUs may be slightly less accurate than the QAs
 278 however, overall the IMU compares very well with the QA. To examine if the amplitude of the
 279 acceleration signal affected the performance of the IMU (with respect to the QA) similar tests were
 280 performed at 50% and 75% of full shaker force output, leading to acceleration signals with
 281 amplitudes of $\pm 2 \text{ m/s}^2$ and $\pm 3 \text{ m/s}^2$ respectively. Plots almost identical to those shown in Fig. 4 were
 282 obtained, with the only difference being that the transfer functions for higher amplitude
 283 acceleration signals decline more gently than shown in Fig. 4(e). Essentially for larger amplitudes of
 284 acceleration the IMUs provide a performance even closer to the performance of the QA. This is to be
 285 expected, the higher sensor noise of the IMU (see section 2) becomes less of an issue for higher
 286 values of acceleration.

287 The signal levels ($\sim \pm 1 \text{ m/s}^2$) and frequencies (0-20 Hz) here are typical of lively footbridges and floors
 288 that are usual applications for modal testing to diagnose vibration serviceability problems and in
 289 these applications the accelerometer in the IMU works well. However, capabilities at lower signal
 290 levels and to identify mode shapes remain to be tested, and these will be examined in subsequent
 291 sections. In particular IMUs must also remain accurately synchronised for the duration of the test so
 292 that modal analysis algorithms can work [30]. The ability of the IMU network to remain synchronised
 293 in laboratory conditions is examined in the next section where IMUs are used to determine the
 294 mode shapes of a laboratory floor structure having high natural frequencies.



295

296 Fig. 3, IMU and QA on shaker.



297

298 Fig. 4, results from shaker test (a) full time history (b) zoomed in view on a portion of the time series,
 299 (c) frequency content of time series shown in (a), (d) zoomed in view of frequency content, (e)
 300 Transfer function between QA and IMU, (f) Magnitude squared coherence between QA and IMU.

301 3.2 Modal test of floor structure

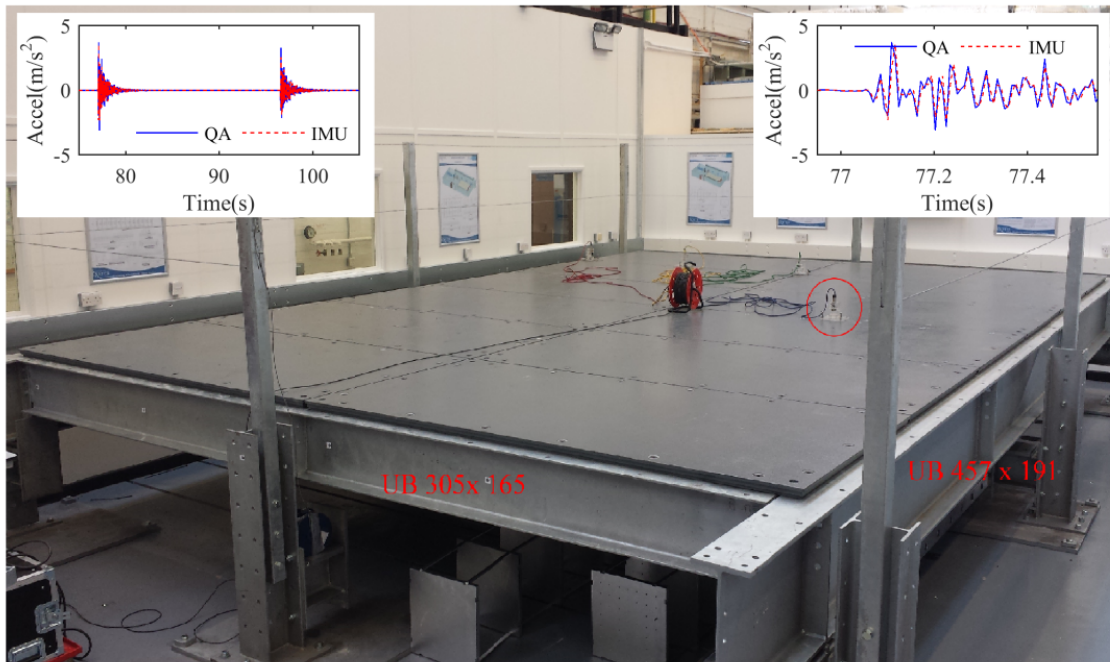
302 3.2.1 Experimental setup for modal test on lab structure

303 The test structure is the 5m x 7.5m steel floor structure shown in Fig. 5, the structure is supported
304 only at the corners. The structure consists of a series of steel plates supported on steel beams. The
305 two longitudinal beams (UB 475x191) span 7.5m between the supports. The transverse beam (UB
306 305x165) are 5.0m long and they span between the longitudinal beams, these beams are indicated
307 in Fig. 5. Finally an internal longitudinal beam (UC 203x203) spans between the two end transverse
308 beams, this beam is under the slab and therefore is not visible in the figure. The slab is formed using
309 42mm thick plates, and these span between the longitudinal beams. The plates are Sandwich Plate
310 System (SPS) plates manufactured by Intelligent Engineering and consist of two metal plates bonded
311 with a polyurethane elastomer core.

312 In total 35 test points were used in the modal survey, the test grid having 5 test points in the
313 transverse location and 7 in the longitudinal direction. The position of the sensor locations can be
314 understood by examining the grid shown in Table 1. On the day of the test only 4 QA accelerometers
315 were available so one accelerometer was left at TP 25 as a reference (circled in Fig. 5) and it
316 remained in this location for the duration of the test. During the test one IMU was 'paired' with each
317 one of the four QA's by simply leaving it on the base plate of the QA as shown in Fig.1, and all of the
318 IMUs were operating in SLM. Then over the course of 12 swipes the 3 (roving) accelerometers roved
319 to the remaining 34 points. For example the photo in Fig. 5 shows the position of the accelerometers
320 for swipe 6 where the reference accelerometer is at test point 25 and the three roving
321 accelerometers are at test points 6, 13 and 20 respectively. For each swipe the structure was excited
322 by a person doing a series of heel drops, typically six heel drops were carried out and each swipe
323 took approximately 4 minutes to record. To excite as many modes as possible the person was
324 standing at the centre longitudinally but slightly off centre transversely. The scanning frequency for
325 both the QA and IMU sensors was 128 Hz. The acceleration recorded at test point 25 due to two
326 consecutive heel drops close to the centre of the floor structure is shown as an insert in the top left
327 of Fig. 5. A zoomed in view of the first heel strike is shown in the insert in the top right of the figure
328 and it can be seen that there is good agreement between the two signals.

329 Finally it should be noted that in a laboratory environment, while it is quicker to collect the data with
330 the IMUs than with the QA's the difference is not so pronounced. This is because in the laboratory
331 there is ready availability of power, there is no need to shelter the logging station, and we are free to
332 run cables wherever we want. However, in the next section it is shown that when collecting data on
333 a road bridge the IMU's prove vastly quicker/easier to use than the QA's.

334



335

336 Fig. 5, Test floor structure in the laboratory and accelerometer locations for swipe 6 of the modal
 337 test.

338

339 3.2.2 Modal identification procedure

340 After the lab testing a sequence of twelve four-minute recordings were available for the QA data.
 341 After the lab test the four IMU's were placed in the docking station and the data from the entire test
 342 was downloaded. Subsequently this was split time-wise into twelve four-minute recordings
 343 corresponding to the twelve QA recordings. The modal analysis procedure used to identify the mode
 344 shapes in the QA and IMU data was exactly the same.

345 The method used is the NExT/ERA operational modal analysis procedure [34]. This is one of several
 346 possible operational modal analysis procedures [35-37] and was used here due to long experience in
 347 its use and implementation in bespoke software [38]. NExT/ERA is now a standard procedure so
 348 only a very brief overview of the procedure as applied to these data is provided below.

349 While NExT/ERA is usually applied to ambient vibration due to broad band random or near-random
 350 excitation (e.g. wind, road traffic) it also works well with induced transient response, and in fact the
 351 transient response to a heel drop resembles the time series generated by the NExT (natural
 352 excitation technique) stage, as input to the ERA (eigensystem realisation algorithm) stage of the
 353 procedure.

354 Each of the twelve recordings was truncated to 200 seconds as five consecutive 40-second frames.
 355 For each swipe a 4x4 cross-spectral density (CSD) matrix was created using the Welch procedure
 356 [39] without overlap or windowing, resulting in twelve CSD matrices corresponding to the twelve
 357 swipes. Subsequently each of these CSD matrices were normalised with respect to the reference
 358 sensor by dividing each frequency line/layer of the CSD matrix by the auto-power of the reference

359 sensor. This normalisation allows the twelve individual CSD matrices to be merged into a single
360 35x35 'global' CSD matrix.

361 Using an inverse Fourier transform the global CSD matrix was transformed to time domain as
362 impulse response functions (IRFs) for the ERA procedure for recover of the modal properties. Based
363 on this, a set of five modes is visible up to 32 Hz. For both the QA and IMU data the NExT/ERA
364 procedure produced a clean set of modes, which are presented in the next section.

365 3.2.3 Results of test on lab structure

366 Using the modal analysis approach described in section 3.2.2 the mode shapes and frequencies
367 shown in Table 1 were obtained. It can be seen that mode shapes calculated from the IMU data
368 agree very well with those calculated from the QA data. This indicates that the IMUs remained
369 synchronised for the duration of this test. In addition, the level of damping calculated is a very good
370 match between the QA and IMU sensors. This demonstrates that under laboratory conditions,
371 where the IMUs remain relatively close together, data collected from them can be used to
372 determine the mode shapes of the structure.

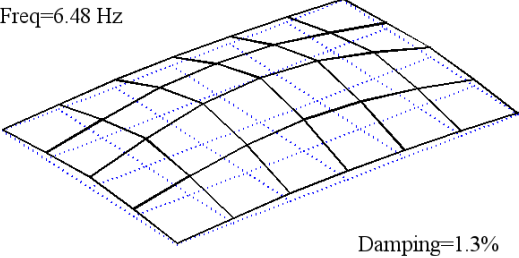
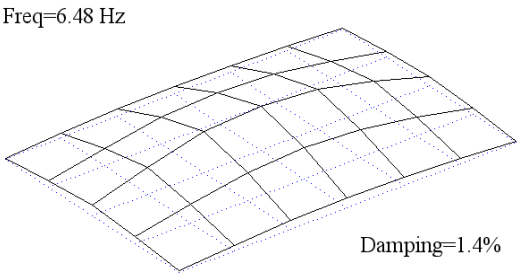
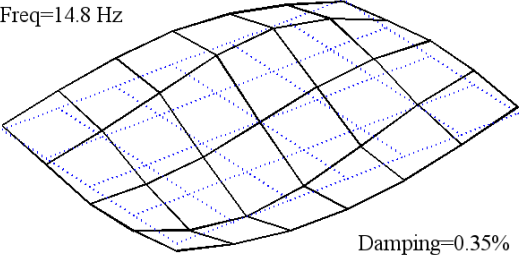
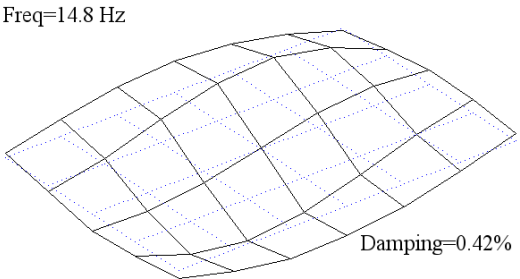
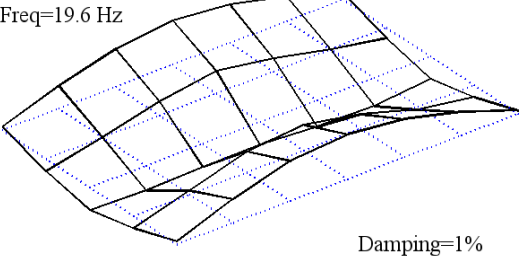
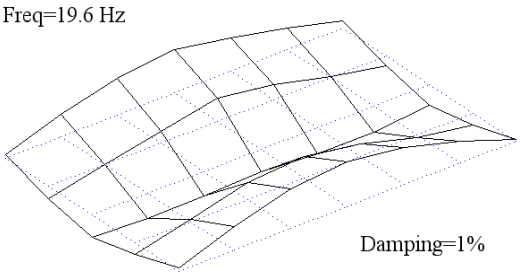
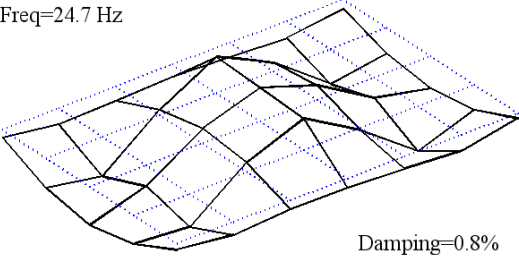
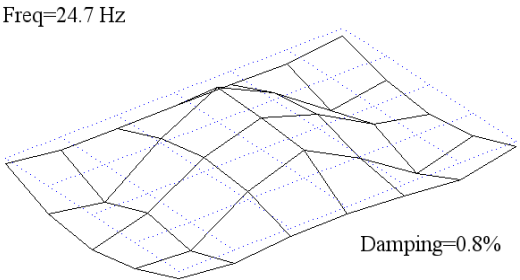
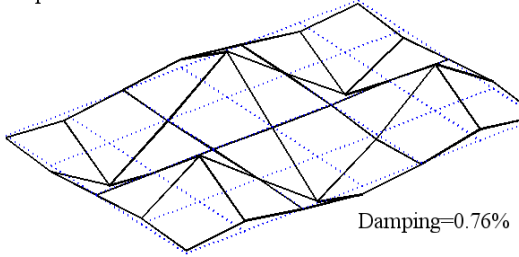
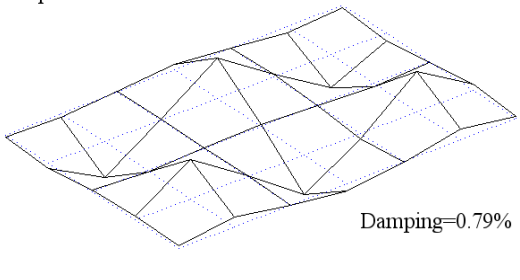
373 Rather than relying on a single numerical indicator such as modal assurance Criteria (MAC), we
374 prefer visual inspection of the mode shapes which can reveal differences that MAC obscures.
375 Inspection of Table 1 shows that all features of the mode shapes are identified equally well using the
376 IMUs.

377 In a laboratory setting where IMUs maintain continuous wireless communication between each
378 other gross synchronisation errors would be prevented so a short measurement is enough to check
379 for minor errors of timing between the IMUs. These would have a proportional greater effect at
380 higher frequencies so the good comparison of the highest frequency modes suggests that there is
381 neither monotonic drift nor small timing variation of any consequence for modal identification when
382 used for testing structures of this scale. However, before further conclusions can be drawn on the
383 applicability of the IMU's for the modal testing of structures it is necessary to test them on real
384 structures in the field. Conditions in the field may be more challenging, e.g. levels of vibration may
385 be smaller and/or the conditions may be such that the sensors lose wireless contact and as a result
386 may lose synchronisation. Therefore field tests on a steel road bridge and a seven story office tower
387 were carried out and are reported in sections 4 and 5 respectively.

388

389 Table 1, Frequencies, damping coefficients and mode shapes for the first 5 vertical modes

Mode No	QA	IMU	% Freq Diff*
---------	----	-----	--------------

1	<p>Freq=6.48 Hz</p>  <p>Damping=1.3%</p>	<p>Freq=6.48 Hz</p>  <p>Damping=1.4%</p>	0%
2	<p>Freq=14.8 Hz</p>  <p>Damping=0.35%</p>	<p>Freq=14.8 Hz</p>  <p>Damping=0.42%</p>	0%
3	<p>Freq=19.6 Hz</p>  <p>Damping=1%</p>	<p>Freq=19.6 Hz</p>  <p>Damping=1%</p>	0%
4	<p>Freq=24.7 Hz</p>  <p>Damping=0.8%</p>	<p>Freq=24.7 Hz</p>  <p>Damping=0.8%</p>	0%
5	<p>Freq=31.1 Hz</p>  <p>Damping=0.76%</p>	<p>Freq=31.1 Hz</p>  <p>Damping=0.79%</p>	0%
* Percentage difference between the IMU frequency and QA frequency			

390 **4.0 Field test on steel road bridge**

391 4.1 Description of Bridge

392 Fig. 6 shows the bridge used in this experiment and a plan view of the bridge is shown Fig. 7. The
393 bridge is a half through steel girder bridge, it spans 36 m and the deck is simply supported. The 7.6 m
394 wide, 200mm deep, concrete deck is supported on a series of 450 mm deep steel beams spanning
395 transversely between the main girders which are approximately 2 m deep.

396
397



398
399 Fig. 6, Bridge used in field test.

400 4.2 Collecting acceleration data

401 This section describes installing a conventional sensing system on a live bridge (section 4.2.1), and
402 the procedure for installing wireless IMUs (section 4.2.2).

403 Using wired accelerometers in the field requires a logging station to be set up and wires installed to
404 connect each sensor to the logging station. Conventional wireless systems described in section 1 still
405 require a logging station but the sensors are connected wirelessly to the logging station for wireless
406 streaming of the data. However, it is not uncommon to have to spend time finding the necessary
407 uninterrupted lines of sight for the wireless system to work properly.

408 So in both a wired arrangement and a conventional wireless system there is (i) a logging station and
409 (ii) a system to transmit data from the sensor to the logging station.. The IMUs requires neither (i)
410 nor (ii) because the data is logged at source and synchronisation is implemented by the sensors
411 communicating with each other to ensure time synchronisation. Not having to install (i) and (ii)
412 makes collecting field data with the IMU's vastly easier. The wired test described in section 4.2.1
413 took one person several days to plan and four people one day to execute. Planning and executing
414 the test with the IMU system (section 4.2.2) took one person approximately 1 day.

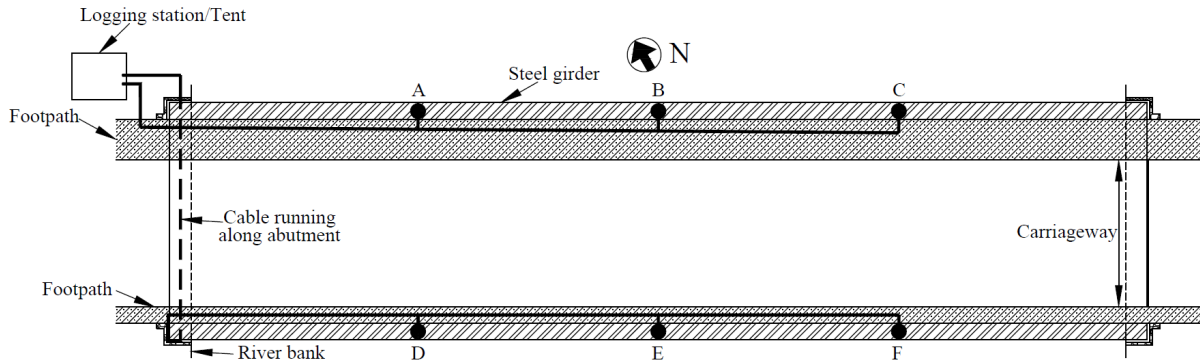
415

416 **4.2.1 Wired system (QAs)**

417 Fig. 7 shows a plan view of the bridge and the accelerometer locations used. Accelerometer
418 locations A, B & C were at the $\frac{1}{4}$ point, mid-span and $\frac{3}{4}$ point of the deck on the north side of the
419 bridge, locations D-F were at the same longitudinal positions on the south side of the deck. The data
420 logging tent was set up at the northwest corner of the bridge and this is indicated in the top left of
421 the figure. The accelerometer at location B is shown in Fig. 8(c), the accelerometer is attached to the
422 underside of the top flange via a magnet, and the signal is carried to the data logger via the cables
423 visible in the image. A schematic of the route taken by the cables is indicated in Fig. 7. Carrying the
424 signal from the sensors on the south side of the bridge to the logger was logistically difficult as it is
425 necessary to run a cable under the bridge deck (along the abutment shelf) which is slow and risky to

426 install when the bridge spans over a river. A view of the logging tent is shown in Fig. 8(a) and the
427 logging equipment used is shown in Fig. 8(b). In total acceleration was recorded for approximately
428 45 minutes and Fig. 8(d) shows the typical acceleration response recorded at sensor location B as a
429 car crossed over the bridge.

430
431



432
433 Fig. 7, schematic of the accelerometer locations A-F and corresponding cabling arrangement.

434
435 Carrying out the test described above takes a significant amount of time with most of the time being
436 spent in the planning phase. The planning phase takes time because (1) installing cabling on a live
437 bridge and erecting a logging station in a public area requires various health and safety permissions
438 be applied for, and (2) the amount of equipment required to be brought to site (sensors, cabling,
439 logging equipment, power source etc.) takes time to organise. But even once on site, setting up and
440 demounting the equipment takes 3-4 people several hours.

441
442
443
444
445
446
447
448
449



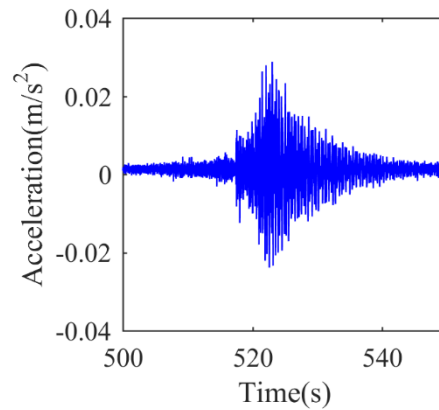
(a)



(b)



(c)



(d)

450

451

452

453

454

455

456

457

458

459

460

461

462

463

464

465

466

467

468

469

470

471

Fig. 8, Test set up for wired test (a) tent for data logging equipment positioned at northwest corner of bridge (b) logging equipment inside the tent, (c) accelerometer attached to underside of girder flange and associated cabling, (d) bridge acceleration response to a passing car

4.2.2 Wireless system (IMUs)

When collecting the data with the IMUs the same accelerometer locations (A-F in Fig. 7) were used. Fig. 9 shows the girder on the south side of the bridge and it can be seen that there is a horizontal steel member running along the length of the girder. The IMUs were attached to the bridge by taping them to this member, and a zoomed in view is shown in the insert of the figure. Mounting the IMUs adjacent to the vertical web stiffeners ensures the sensor is only picking up global bridge vibrations rather than local vibrations of the horizontal member. IMUs mounted at locations F, E & D are indicated in the figure. Acceleration was recorded for 45 minutes and acceleration response recorded by the IMU at mid-span due to the passage of a car looked very similar to the signal shown in Fig. 8(d). As collecting the data with the IMU's essentially requires just 6 sensors to be mounted locally on the bridge the health and safety permissions are minimal, and therefore very quickly/easily obtained. The planning phase is practically non-existent as the only equipment required to be brought to site are six IMU's that can be carried in a coat pocket. Once on site one person can install and (once the test is complete) demount the sensors in approximately 10 and 5 minutes respectively. So relative to the man hours required to collect the data with a wired system collecting the data with the IMUs takes vastly less time. The mode shapes identified by both systems are presented in the next section.



472

473 Fig. 9, IMUs deployed at sensor locations F, E & D (see Fig. 7), insert shows how IMUs were simply
474 taped to the horizontal member adjacent to the vertical web stiffener.

475 4.3 Mode shapes from road bridge

476 The modal identification procedure described in section 3.2.2 was implemented to identify the mode
477 shapes from both the QA and IMU data and the results are shown in Table 2. Similar to the floor
478 structure the mode shapes and frequencies calculated using the IMU sensors compares very well
479 with those calculated using the wired QA system. There are some differences in the frequencies
480 observed but it should be noted that the data for both systems were collected on different days and
481 the day of the IMU test was colder, so some small differences in frequencies is to be expected [40].
482 The results shown in table 2 demonstrates primarily two things, firstly when the amplitude of
483 acceleration is in the region of $\pm 0.1 \text{ m/s}^2$ or greater the IMUs will be able to capture the vibration.
484 Secondly when contained in an open area (18 m x 9 m) the IMUs remain sufficiently well
485 synchronised to capture the mode shapes. This is believed to be because the distance between
486 individual IMUs is sufficiently small that mesh synchronisation algorithm remains working. To further
487 explore the capabilities of the IMUs for modal testing in the next section more challenging test
488 environment is examined in the form of a 7 storey office tower. In the tower the vibrations are less
489 than 0.1 m/s^2 and the IMUs will be separated by walls and concrete floors.

490

491

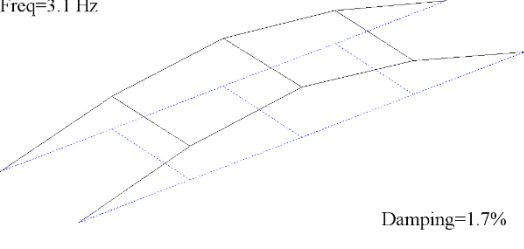
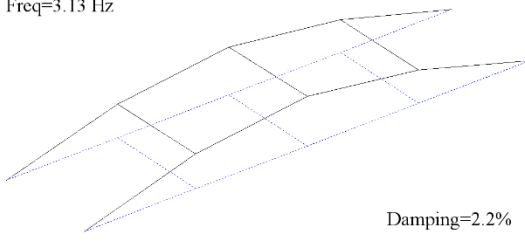
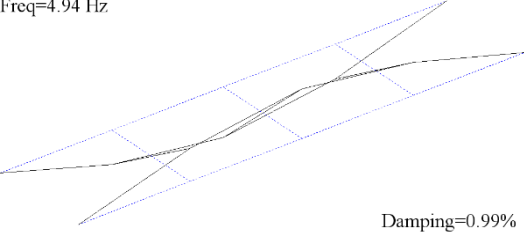
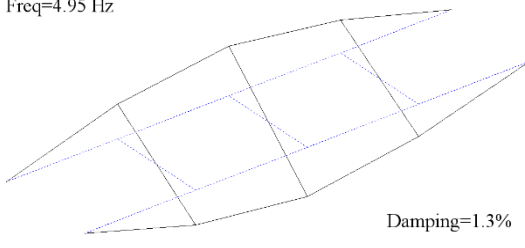
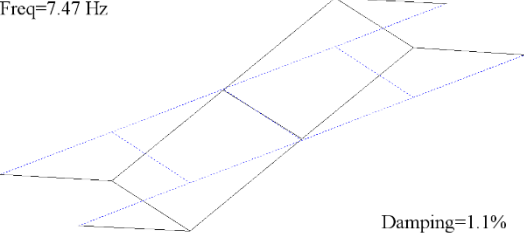
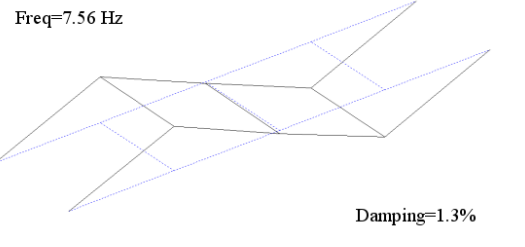
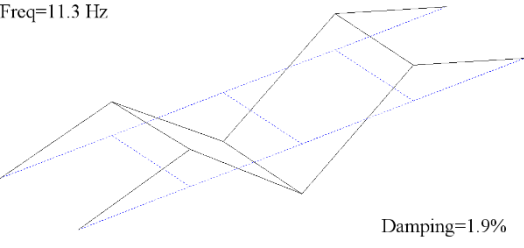
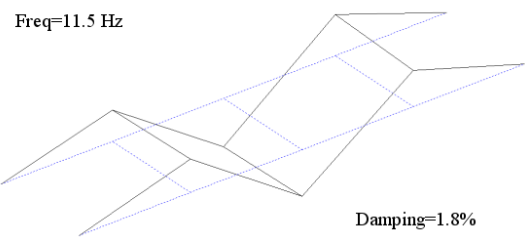
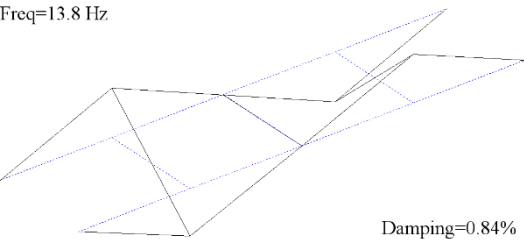
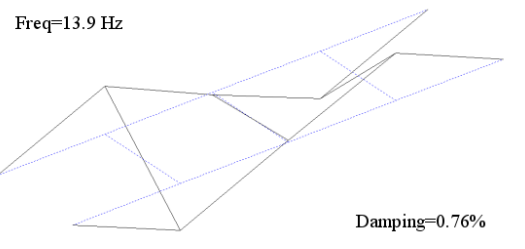
492

493

494

495

496 Table 2, Frequencies and mode shapes for the first 5 vertical modes

Mode No	QA	IMU	% Freq Diff*
1	<p>Freq=3.1 Hz</p>  <p>Damping=1.7%</p>	<p>Freq=3.13 Hz</p>  <p>Damping=2.2%</p>	0.95%
2	<p>Freq=4.94 Hz</p>  <p>Damping=0.99%</p>	<p>Freq=4.95 Hz</p>  <p>Damping=1.3%</p>	0.20%
3	<p>Freq=7.47 Hz</p>  <p>Damping=1.1%</p>	<p>Freq=7.56 Hz</p>  <p>Damping=1.3%</p>	1.20%
4	<p>Freq=11.3 Hz</p>  <p>Damping=1.9%</p>	<p>Freq=11.5 Hz</p>  <p>Damping=1.8%</p>	1.77%
5	<p>Freq=13.8 Hz</p>  <p>Damping=0.84%</p>	<p>Freq=13.9 Hz</p>  <p>Damping=0.76%</p>	0.72%
* Percentage difference between the IMU frequency and QA frequency			

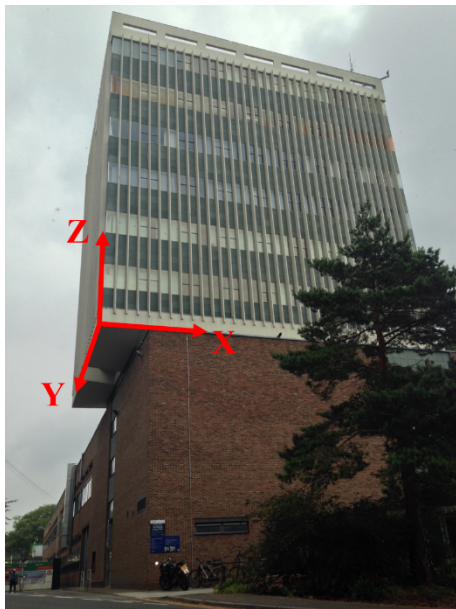
497

498

499 5.0 Field test on 7 storey concrete office tower

500 5.1 Description of tower

501 The building used in the test is shown in Fig. 10. Structurally the tower is a little unusual in that
502 floors 2-7 have slightly larger plan dimensions than the lower floors. This can be seen in Fig. 10
503 where the second floor overhangs the lower floors. The plan dimensions of floors 2-7 is 22m x 16m
504 in the x and y directions respectively. For ease of visualisation horizontal x and y axes are indicated in
505 the figure. In Fig. 10 it can be seen that the ground floor and first floor of the building are much
506 longer in the y-direction. For the purposes of this test only tower vibrations are recorded, i.e. no
507 data is recorded in other parts of the building. In total the tower has 10 floors, namely; basement,
508 ground floor, first floor, mezzanine floor, second floor, and floors 3-7. For visualisation purposes a
509 3D schematic of the building is shown in Fig. 12, however for simplicity, the overhang at the 2nd floor
510 is not indicated. Lateral stability for the tower is provided by a reinforced concrete stairwell and lift
511 core. A schematic of the floor plan for floors 7, 5 and 3 are shown in Figs. 11(a-c) respectively.



512

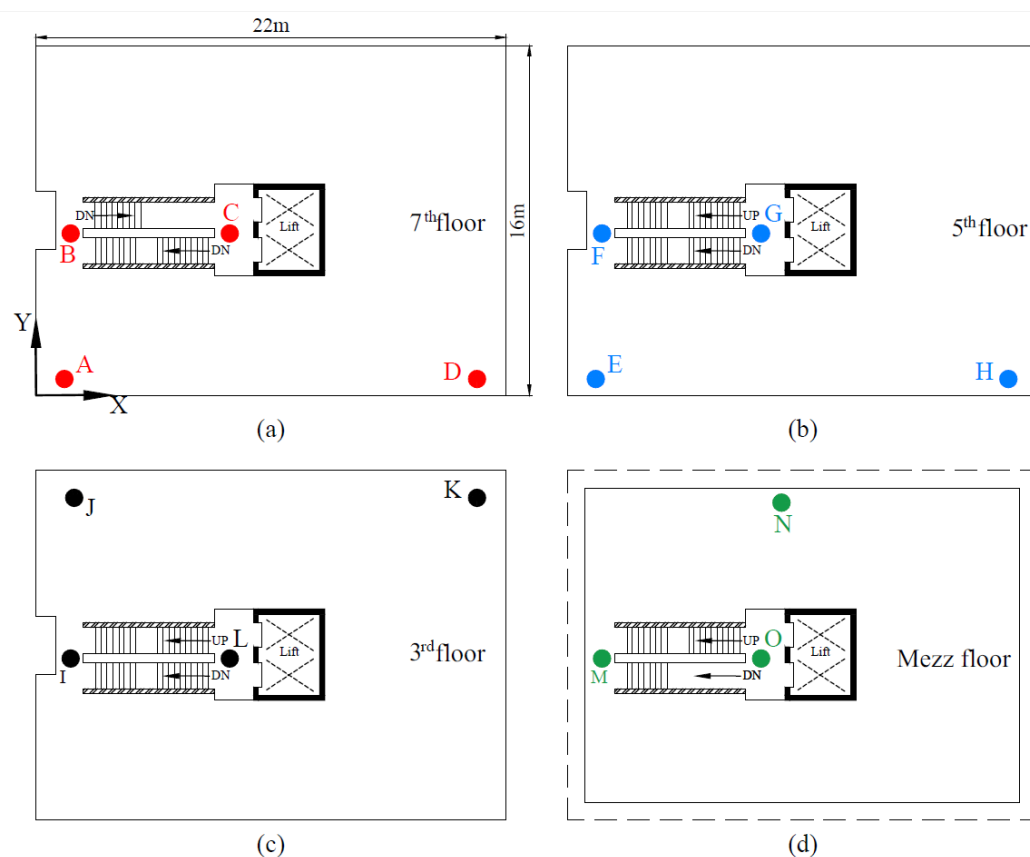
513 Fig. 10, Tower used in test.

514

515 5.2 Collecting acceleration data

516 In this test acceleration is recorded four separate floors, namely floors 7, 5, 3 and the mezzanine
517 floor and the location of the test points used on each floor are indicated in Fig. 11 using circular dots.
518 The schematic in Fig. 11 does not show the room layout in the building (i.e. non-structural walls
519 have been omitted) and as a result the irregular test points (on each floor) initially look a little odd.
520 However, on the night of the test the monitoring team did not have access to all parts of the building
521 and therefore accelerometers had to be located where access was permitted. In total acceleration
522 was recorded at fifteen different test points in the building labelled A-O in Fig. 11, four test points on
523 each of floors 7, 5, and 3, and three test points on the Mezzanine floor.

524



526

527 Fig. 11, schematic floor plans of the tower and test points used in modal test (a) 7th floor, (b) 5th
 528 floor, (c) 3rd floor, (d) mezzanine floor.

529 Each test point required two QA accelerometers to measure acceleration in the x and y directions,
 530 and one IMU, (the IMU has a triaxial accelerometer so only one IMU is required per test point). Both
 531 the QA's and the IMU were scanning at 128 Hz and the typical accelerometer arrangement at a test
 532 point is shown in Fig. 13(a). Due to the limited number of sensors available the data was collected in
 533 a number of 'swipes'. Table 3 gives a summary of the test points where acceleration was being
 534 recorded during a given swipe. It can be seen in the right hand column of Table 3 that test point A is
 535 included in all four swipes, this is to allow the data from the different swipes to be 'glued' together
 536 in post processing. To allow a 3D visualisation of where test points A-O are located in the building
 537 the approximate position of the test points on each floor is shown in Fig. 12. Test point A on the 7th
 538 floor is where the reference accelerometers are located.

539 Setting up the sensors for each swipe took in the region of 35-45 minutes and during each swipe
 540 acceleration was recorded for 24 minutes. In an effort to minimise any time drift in the IMU signals,
 541 just before the start of each swipe the five IMUs used in the test were brought together for at least
 542 two minutes to allow mesh synchronisation to occur, then they would be distributed to the test
 543 points for that swipe. Carrying out the test this way ensured that at least at the start of every swipe
 544 the IMUs were synchronised. The observed performance of the IMU's with respect to time drift is
 545 discussed in detail in the next section. For ease of cabling the logging station was set up on the 3rd
 546 floor and is shown in Fig. 13(b).

547 The fact that the QA's need a logging station means that cables need to be ran through people's
 548 offices and more problematically through public corridors and stairwells, to get the accelerometer
 549 signals to the logging station. Aside from the time it takes to, (a) install the cables, (b) secure them to
 550 minimise the trip hazard, and (c) remove them after the test. A significantly larger amount of time is
 551 spent preparing Health and Safety method statements and agreeing with the building operator safe
 552 routes for the cabling etc. For the IMUs (a)-(c) are simply not necessary, and as a result the time
 553 required to prepare and agree the method statements and risk assessments for a purely IMU test
 554 would only be a fraction of the time for the corresponding wired test.

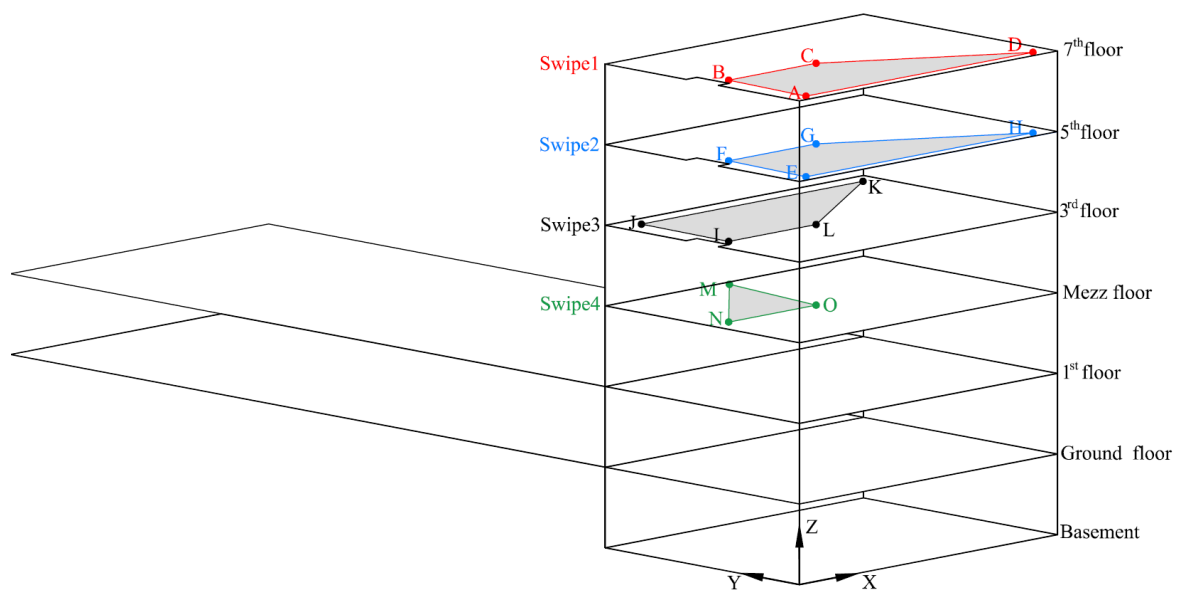
555 Table 3, Test points in each of the four swipes

Swipe No	Floor where most of the Test points are	Test points in the swipe*
1	7 th floor	A , B, C, D
2	5 th floor	A , E, F, G, H
3	3 rd floor	A , I, J, K, L
4	Mezzanine floor	A , M, N, O

**Test point where reference accelerometers located is indicated in bold*

556

557



558

559 Fig. 12, 3D schematic of the tower with the test points on each floor indicated.



(a)



(b)

560 Fig. 13, (a) two QA accelerometers and one IMU sensor at test point A on the 7th floor (b) data
561 acquisition

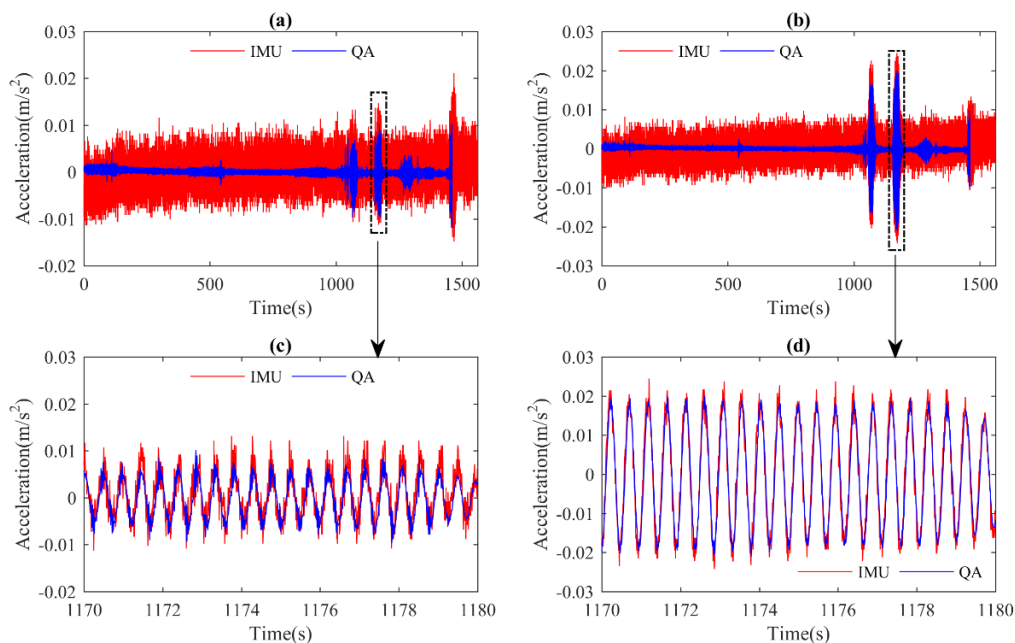
562 Fig. 14 shows the signals recorded at test point A (the reference location on the 7th floor) during
563 swipe 1, with parts (a) and (b) showing the acceleration in the x and y directions respectively. The
564 first thing to notice about Figs. 14 (a) and (b) is that the noise floor for the QA's is much lower than
565 for the IMUs, reflecting the result shown in Fig. 2. On the night of the test there was almost no wind
566 so the tower was moving very little and as a result in the first 750 seconds (i.e. the first half) of the
567 swipe the IMU signal is essentially just noise. However, the noise floor of the QA accelerometer is
568 sufficiently low that it is picking up the tower vibrations. The difference in the performance of the
569 both sensors in the first 750 seconds can be seen more clearly in the frequency domain. Figs. 15 (i) &
570 (ii) respectively show the result of analysing the first 750 seconds of the signals shown in Figs. 14 (a)
571 & (b) with the Welch method, window lengths of 120 seconds with a 50% overlap were used. It can
572 be seen in Figs. 15 (i) & (ii) that the QA's are identifying frequencies of 2.5 Hz and 2.1 Hz in the x and
573 y directions respectively but that the IMU is not capturing these frequencies.

574 In an attempt to excite the tower sufficiently that the magnitude of the vibrations would be above
575 noise floor of the IMUs it was decided to try excite the structure with three people stepping laterally
576 from foot to foot at the building frequency. To excite a lateral frequency of 2.1 Hz required the
577 authors to step laterally at a rate of 4.2 steps per second. To achieve this rhythm an audio
578 metronome was set to 252 beats per minute and the three authors stepped/jumped at this rate on
579 the 7th floor of the building. Fig. 16 shows an image of the authors jumping, note in this image the
580 authors shoulders are parallel with the y axis of the building. The large pulses in acceleration at
581 approximately 1100 seconds in Fig. 14 (a) & (b) is as a results of this jumping. The zoomed in view
582 shown in Fig. 14 (c) & (d) shows clear sinusoidal signals for both the IMUs and QAs and it can be seen
583 that the signals from the IMUs agree very well with the signals from the QA's.

584 Once the 2.1 Hz mode had been excited the authors realigned so that they were standing one
585 behind the other but now their shoulders were parallel with the buildings x axis. To excite a

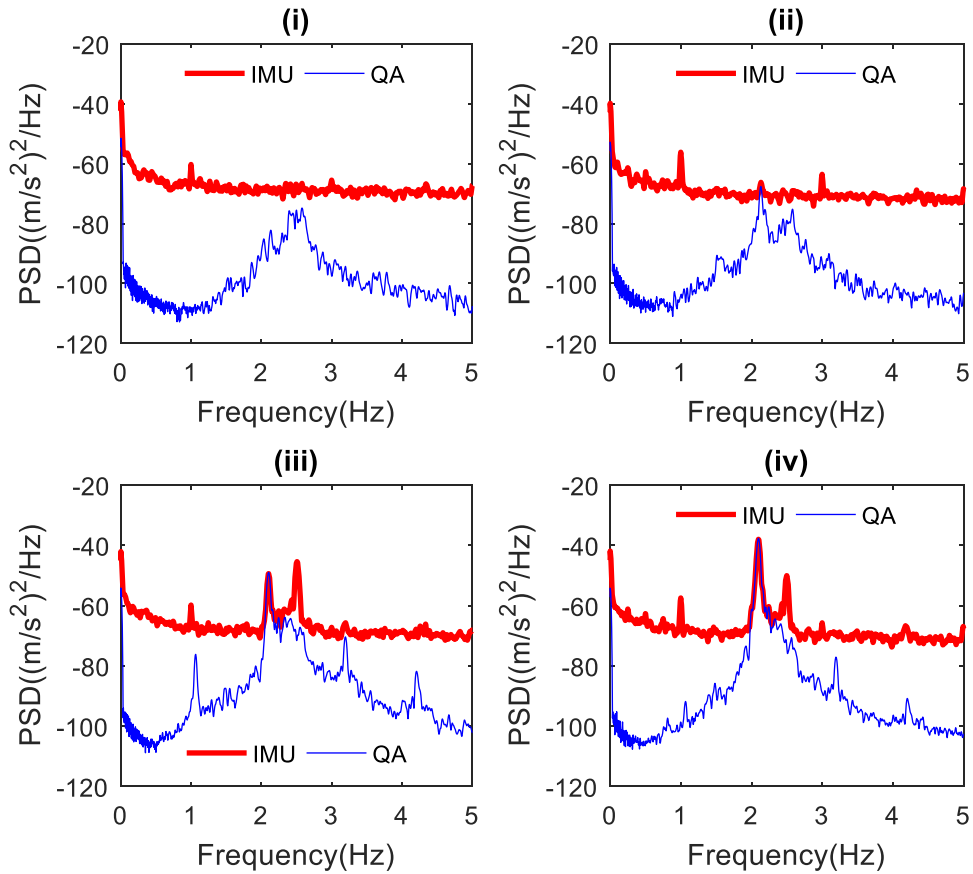
586 frequency of 2.5 Hz required the authors to step at a rate of 5 steps per second. The pulse in IMU
 587 acceleration visible in Fig. 14 (a) & (b) at approximately 1400 seconds are as a result of this
 588 stepping/jumping. However, it should be noted that the authors found 5 steps per second towards
 589 the upper end of what was physically possible and it would be impossible to excite higher modes
 590 using this technique. The reason the IMU time series in Fig. 14(a) and Fig. 14(b) is a little longer than
 591 the QA time series is that the data logger recording the QA signals had been programmed to
 592 automatically stop recording after 24 minutes, so the QAs just missed the jumping/stepping in the x-
 593 direction.

594 Figs. 15(iii) and (iv) respectively show the frequency content of the signals that were recorded during
 595 the jumping phase of the test, i.e. the signals in the latter half of Fig. 14(a) and (b), from 750 seconds
 596 onwards. Unlike Figs. 15(i) and (ii) when the IMU data were unable to capture the building
 597 frequencies in Figs. 15(iii) and (iv), the building frequencies are clearly evident in the IMU data. Once
 598 it had been shown that the IMU's could capture the tower frequencies provided the building was
 599 excited by humans jumping this procedure was also followed for Swipes 2-4. At the end of each
 600 swipe all five IMUs were brought together to allow them to resynchronise if they had lost
 601 synchronisation. the mode shapes identified from both the QA and IMU data are presented section
 602 5.4.



603
 604 Fig. 14 Acceleration recorded at reference location (test point A) during swipe 1, (a) acceleration in
 605 x-direction (b) acceleration in y-direction, (c) zoomed in in view at 1170 seconds (d) zoomed in in
 606 view at 1170 seconds

607



608

609 Fig. 15, Frequency content of the signals shown in Fig. 14, (i) frequency content of the first 750
 610 seconds of acceleration data shown in Fig. 14(a), (ii) frequency content of the first 750 seconds of
 611 acceleration data shown in Fig. 14(b), (iii) Frequency content of second half of the IMU acceleration
 612 signal shown in Fig. 14(a) i.e. after 750 seconds, (iv) Frequency content of second half of the IMU
 613 acceleration signal shown in Fig. 14(b) i.e. after 750 seconds.

614



615

616 Fig. 16, three of the authors stepping laterally to a predetermined beat on the 7th floor to excite
617 building motion.

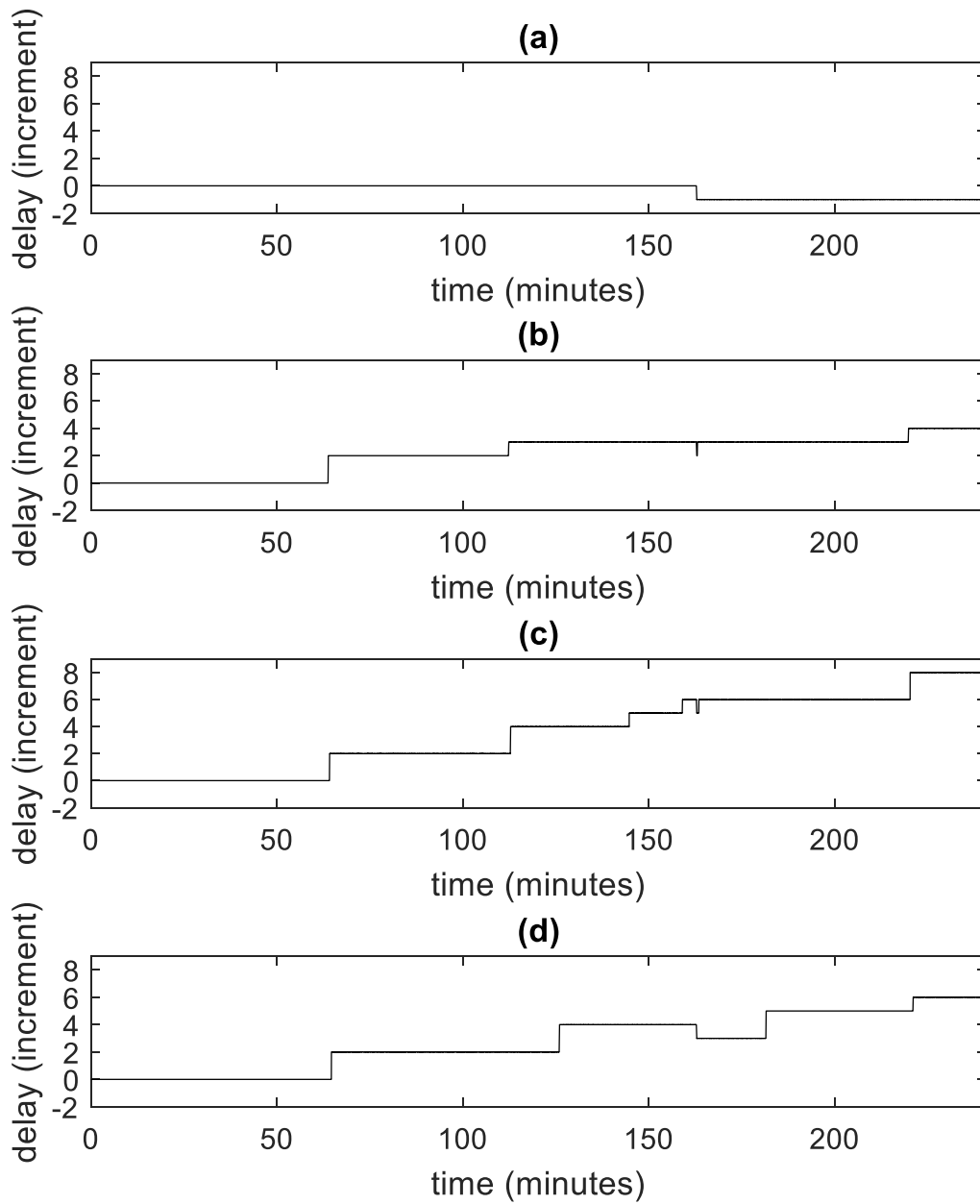
618

619 5.3 IMU Synchronisation

620 Prior to carrying out modal identification on the tower data, the amount of time drift that occurred
621 between the different IMUs was investigated. As explained in Section 2.2 each IMU has its own
622 internal clock and the data recorded at a given time instant is time stamped against the time on the
623 internal clock. When operating in SLM, if the IMUs remain within range of each other the timing of
624 each internal clock is adjusted according to a probabilistic model, so the time on all the clocks
625 remains identical and therefore the data from each IMU is synchronised. Once an individual IMU
626 sensor is out of range of its companions in the network, then the clock in that IMU is running
627 independently so there is a possibility that it will start to run slightly ahead, or slightly behind the
628 internal clocks of the other IMUs. The likelihood of the clock of the isolated IMU starting to run
629 slightly ahead/behind the clocks of the other IMUs is increased if the isolated sensor is placed in a
630 significantly different temperature to the other IMUs in the network. Once all the IMUs are reunited,
631 i.e. that all five are within wireless range of each other, the probabilistic timing model will engage
632 and identify what it considers the 'correct' time. Then the clock of any IMU not reading the correct
633 time will be adjusted forward or backwards such that it is reading the correct time. This occasional
634 correcting of the time on the internal clock can be seen in post processing by examining the time
635 stamps from the IMUs. The IMUs were scanning at 128 Hz so consecutive clock readings
636 increase by 0.0078125 seconds, henceforth known as one time increment. However, if the clock in
637 an isolated IMU has started to run a little 'slow', when the isolated IMU is brought back to the rest of
638 the network it's clock will increment by two (or possibly three) time increments in a single step to
639 bring that clock into line with the other clocks in the network. Alternatively if the clock in the
640 isolated IMU had started to run 'fast', when it is reunited with its companions in the network the
641 timestamp may increment by zero between consecutive steps, or possibly even show a negative
642 increase if it is two or more time increments out of synchronisation.

643 While the procedure described above (i.e. looking at the time stamps of individual IMUs) can be
644 used to identify potential drift. When dealing with a network of five IMUs it is more meaningful to
645 take the time stamp from one IMU as the reference, and compare the timestamps of the other four
646 IMUs to the reference timestamp. Fig. 17 shows the result of carrying out such an exercise. IMU
647 No 5 was taken as the reference and its timestamp was compared to the timestamps of IMUs No's 1-
648 4 and the result of this comparison is shown in Figs. 17(a-d) respectively. It should be noted that the
649 IMUs were recording from the start of the test until the end, i.e. IMU recording is not stopped
650 between swipes, instead the swipe data (for the four individual swipes) is cut from the total IMU
651 time series in post processing. In Fig 17(a) it can be seen that in total the IMUs were recording for
652 approximately 240 minutes and that in this period IMU No 1 only drifted from IMU No 5 by one time
653 increment and this occurred after 163 minutes. Parts (b), (c) and (d) of the figure also show some
654 drift at 163 minutes. As described in section 5.2, all five IMUs are all together at the start of a swipe
655 for at least two minutes, and the steps/drifts apparent at 163 minutes is evidence of the
656 probabilistic timing model 'correcting' the time on the internal clocks when the IMUs are reunited
657 after a period of separation for one or more of the IMUs. Other occasions where a step change is
658 observed in the timing of multiple sensors occur at 64 minutes and 112 minutes. Each of the swipes
659 were 24 minutes long, and it can be seen from Fig. 17 that in any given 24 minute period there is
660 never more than two increment drift in the internal clocks of the IMUs. This equates to a maximum
661 drift of approximately 0.0156 seconds ($2 * 0.0078125 \approx 0.0156$). When one is dealing with frequencies
662 less than 10Hz (period ≥ 0.1 seconds) even if an individual IMU goes out of synchronisation with the
663 other sensors in the network by one time step (0.0078 s) or even two time steps (0.0156 s) over the
664 course of a 24 minute swipe it effects the phase very little and as a result the mode shapes will still
665 be correct. The timestamps of the individual IMUs were also checked after the modal test on the
666 bridge (Section 4) however, for the bridge test there were zero slips evident. This is believed to be
667 due to the fact that during the bridge test the IMUs were sufficiently close together to maintain
668 mesh synchronisation in SLM for the duration of the bridge test.

669



671

672 Fig. 17 Variation between the internal clock of the reference IMU (IMU No 5) and the internal clocks
 673 of the other four IMUs in the network (a) Difference between the reference clock and IMU No 1, (b)
 674 Difference between the reference clock and IMU No 2, (c) Difference between the reference clock
 675 and IMU No 3, (d) Difference between the reference clock and IMU No 4.

676

677

678

679 5.4 Mode shapes from tower

680 Having satisfied ourselves that synchronisation will not be a significant problem. The modal
681 identification procedure described in section 3.2.2 was implemented to identify the mode shapes
682 from both the QA and IMU data and the results are shown in Table 4. The stick model in Table 4 can
683 be understood if the sensor layout in Fig. 12 is examined. For modes 1 and 2 the mode shapes and
684 frequencies calculated using the IMU sensors compare very well with those calculated using the
685 wired QA system. However, mode shape 3 is not correctly identified from the IMU data. This may
686 have been because the amplitudes of vibration associated with the third mode were simply so small
687 that they were not detected properly by the accelerometer in the IMU, or it may be that for higher
688 frequencies and therefore lower periods of vibration are more sensitive to time drift between
689 individual IMUs if mesh synchronisation is lost during the swipe. However, the fact that modes 1 and
690 2 are identified correctly in the IMU data is relatively impressive for two reasons. Firstly even with
691 the jumping the magnitude of the acceleration was still quite small with the maximum amplitudes
692 on the 7th floor in the region of 0.01 - 0.02 m/s² with even smaller amplitudes on the lower floors.
693 Secondly for swipes 2-4 there were significant distances and obstructions between the IMUs on the
694 floor being measured and the reference IMU on the 7th floor.

695 It is important to note that without having the QAs on site the night of the test it would have been
696 very difficult for the authors to know what frequencies to jump at to excite the structure. If the
697 authors only had IMU's on the night they would have had to jump at a series of different frequencies
698 in the range of frequencies expected for the building, to see which provide the best excitation and
699 this would have been very slow. However, as noted earlier on the night of the test the weather was
700 extremely calm so a small follow up test was carried out on a windy night to see if the IMUs could
701 capture the structural frequencies (without anyone jumping), and the results of this test are briefly
702 reported in the next section.

703

704

705

706

707

708

709

710

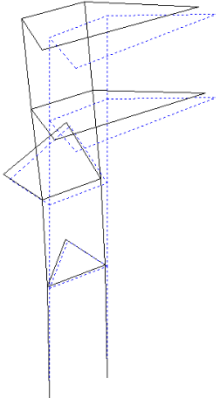
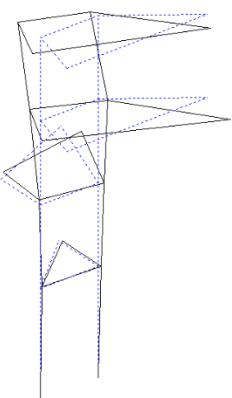
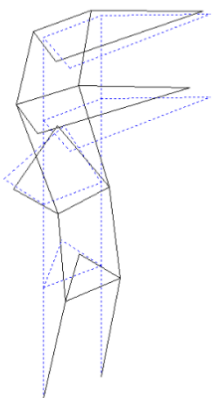
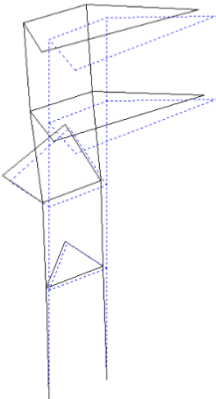
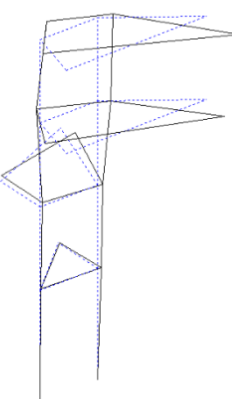
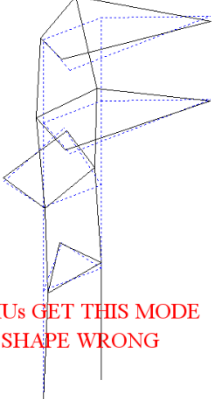
711

712

713

714

715 Table 4, Frequencies, damping coefficients and mode shapes for the first 3 tower modes

	Mode 1	Mode 2	Mode 3
QA	<p>Freq=2.11 Hz</p>  <p>Damping=0.44%</p>	<p>Freq=2.5 Hz</p>  <p>Damping=0.68%</p>	<p>Freq=10.8 Hz</p>  <p>Damping=0.071%</p>
IMU	<p>Freq=2.11 Hz</p>  <p>Damping=0.3%</p>	<p>Freq=2.52 Hz</p>  <p>Damping=0.4%</p>	<p>Freq=10.7 Hz</p>  <p>IMUs GET THIS MODE SHAPE WRONG</p> <p>Damping=0.51%</p>
	0% difference between IMU and QA Frequency	0.79% difference between IMU and QA Frequency	0.93% difference between IMU and QA Frequency

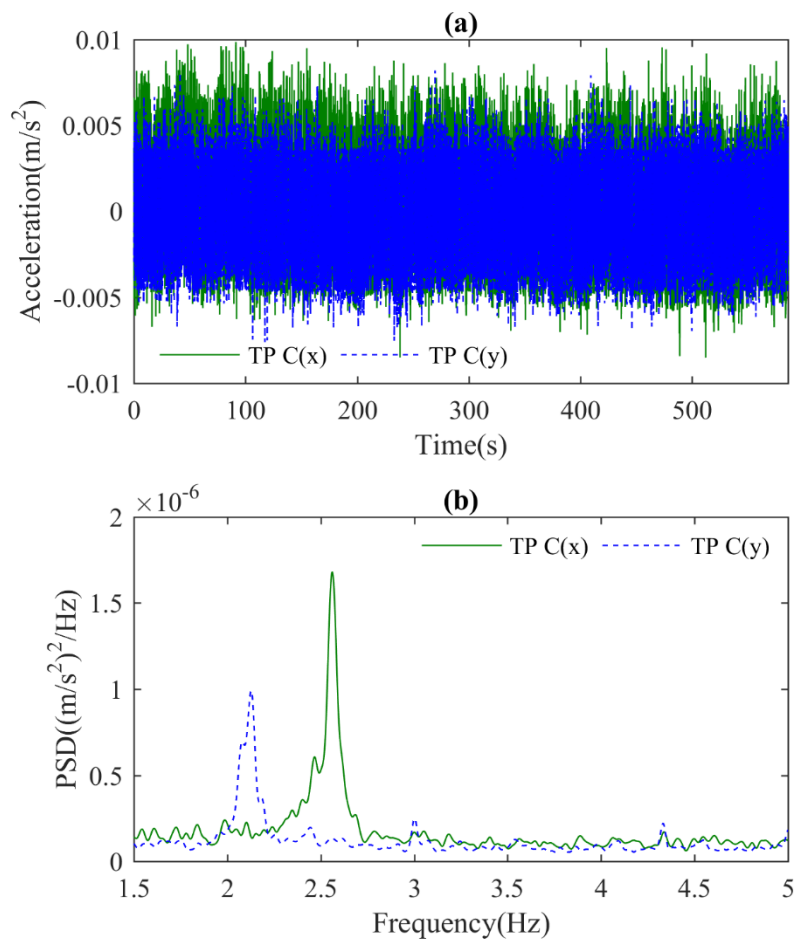
716

717

718 5.5 Limited testing on windy night

719 To see if the IMUs might be able to pick up the building frequencies without people jumping, a
 720 limited test with just one IMU was carried out on a night with winds of approximately 20 mph. The
 721 IMU was positioned on the 7th floor at test point C indicated in Fig. 11(a). Fig. 18(a) shows the
 722 acceleration recorded in the x and y directions as solid and dashed plots respectively. Fig. 18(b)
 723 shows the frequency content of the signals between 1.5 and 5 Hz and it can be seen that the
 724 structural frequencies at 2.1 and 2.5 Hz are clearly visible. Therefore when there is sufficient wind to
 725 excite the structure the IMUs are able to pick up the building frequencies without specific human
 726 excitation.

727



728

729 Fig. 18, Data recorded at test point C on the 7th floor on a night when there was 20 mph wind (a)
 730 time series data, (b) frequency content of acceleration data shown in (a).

731 **6.0 Discussion and conclusions**

732 In this study it was found that the mode shapes identified for the three structures using IMU
 733 acceleration data, were very similar to the corresponding mode shapes identified from the QA
 734 acceleration data. Admittedly for the modal test of the concrete office tower there were some
 735 instances where the QAs were superior but these aspects are further discussed below.

736

737 For the floor structure in the laboratory the IMUs were never more than a few meters apart so no
 738 problems with synchronisation were envisaged and indeed this proved to be the case as the IMUs
 739 performed just as well as the QAs. In the laboratory there was ready availability of power, the
 740 logging station could be set up wherever was convenient and there was no restrictions on where
 741 cables could be ran. Therefore while the IMUs were still quicker to set up than the QAs the
 742 difference was not that pronounced and any time advantages for the IMUs in the set up were at
 743 least partially offset by the extra time required in post processing to cut the data for the 12 swipes
 744 from the total IMU time record.

745

746 However, the test on the steel road bridge really highlighted the potential benefits of the IMUs. Two

747 of the basic requirements when setting up a logging station are electrical power and shelter from the
748 elements. Unlike in a building where these things are readily available, on a bridge site these need to
749 be provided/installed and this takes significant time. Installing the necessary cabling also takes a
750 significant amount of time for three principle reasons;

751 (i) bridge remaining open: during a modal test on a bridge, the bridge will normally remain open to
752 vehicle and pedestrian traffic which places limitations on where cables can be placed, thereby
753 forcing the tester to position the cables in zones with more difficult access, which slows the process
754 down,

755 (ii) length of cable required: the physical size of a real bridge means that tens to hundreds of meters
756 of cable needs to be installed,

757 (iii) challenging access: depending on the height of the deck, what passage the bridge is crossing,
758 limited access to abutments, revetments etc. means it can be difficult/slow to get to the places
759 cables need to be installed.

760 As a result planning and executing the wired test took over one hundred man hours, gathering the
761 same information with the IMUs took approximately ten man hours. After processing the data, the
762 mode shapes from the IMU data were the same as the mode shapes from the QA data. This shows
763 that for the bridge tested the accelerometers in the IMUs were sensitive enough to accurately
764 capture the vibrations and that synchronisation between the IMUs was adequate.

765
766 The structure where the IMUs struggled a bit was the tower. Prior to the tower test the author's
767 primary concern was that in the tower, the IMUs would not have clear lines of sight between each
768 other for wireless communication and therefore one or more sensors might drift (in time) significantly
769 from the others and as a result the IMU signals might not be time synchronised. However, this did
770 not prove to be such an issue. Instead it was found that for very low levels of vibration the noise
771 floor in the IMUs accelerometer is simply too high to allow accelerations to be identified so it was
772 necessary for the authors to artificially induce acceleration at a level high enough for the IMUs to
773 detect it. If the test had been carried out on a windy night it appears from section 5.5 that the IMUs
774 would not need human induced vibrations as the wind is sufficient to excite the structure. Essentially
775 the tower test showed that the primary limitation of the IMUs for structural modal testing is the
776 quality of the accelerometer rather than issues with synchronisation.

777
778 From the three structures tested it was shown that over the course of a 20-30 minute swipe
779 (commonly used for a modal test on a structure) the IMUs did not drift significantly in time. This
780 means that if a more sensitive accelerometer was used they really could be very useful for structural
781 modal testing, particularly on bridge sites. However, if one was going to change the accelerometer it
782 would make sense to make the units a little bigger, and install the hardware necessary to increase
783 the range of the wireless capabilities so that the sensors could remain in wireless communication
784 over longer distances and therefore remain mesh synchronised.

785

786 **Acknowledgements**

787 The research leading to these results has received funding from the People Programme (Marie Curie
788 Actions) of the European Union's Seventh Framework Programme (FP7/2007-2013) under grant
789 agreement n° 330195. The authors would also like to acknowledge the Bridge Section of The
790 Engineering Design Group of Devon County Council led by Kevin Dentith BSc, CEng, FICE, for their
791 support and assistance with this work.

792 **References**

- 793 [1] P. Moyo, J.M.W. Brownjohn, P. Omenzetter, Highway bridge live loading assessment and load
794 carrying estimation using a health monitoring system, *Struct. Eng. Mech.* 18 (2004) 609–626.
- 795 [2] F.N. Catbas, T. Correa-Kijewski, A.E. Aktan, *Structural Identification of Constructed Systems.*
796 *Approaches, Methods and Technologies for Effective Practice of St-Id.*, ASCE, 2013.
- 797 [3] S. Jang, H. Jo, S. Cho, K. Mechitov, J. a Rice, S.H. Sim, H.J. Jung, C.B. Yun, B.F. Spencer, G. Agha,
798 *Structural health monitoring of a cable-stayed bridge using smart sensor technology:*
799 *deployment and evaluation*, *Smart Struct. Syst.* 6 (2010) 439–459.
800 doi:10.12989/sss.2010.6.5_6.439.
- 801 [4] S. Jang, S.-H. Sim, H. Jo, B.F. Spencer Jr, Full-scale experimental validation of decentralized
802 damage identification using wireless smart sensors, *Smart Mater. Struct.* 21 (2012) 115019.
803 doi:10.1088/0964-1726/21/11/115019.
- 804 [5] G.L. Smidt, R.H. Deusinger, J. Arora, J.P. Albright, An automated accelerometry system for gait
805 analysis, *J. Biomech.* 10 (1977) 367–375. doi:10.1016/0021-9290(77)90009-4.
- 806 [6] H.J. Luinge, P.H. Veltink, Measuring orientation of human body segments using miniature
807 gyroscopes and accelerometers, *Med. Biol. Eng. Comput.* 43 (2005) 273–282.
808 doi:10.1007/BF02345966.
- 809 [7] F. Brunetti, J.C. Moreno, A.F. Ruiz, E. Rocon, J.L. Pons, A new platform based on IEEE802.15.4
810 wireless inertial sensors for motion caption and assessment, in: *Int. Conf. IEEE Eng. Med. Biol.*
811 *Soc.*, 2006: pp. 6497–6500.
- 812 [8] M. Bocian, J.M.W. Brownjohn, V. Racic, D. Hester, A. Quattrone, R. Monnickendam, A
813 framework for experimental determination of localised vertical pedestrian forces on full-scale
814 structures using wireless attitude and heading reference systems, *J. Sound Vib.* 376 (2016)
815 217–243. doi:10.1016/j.jsv.2016.05.010.
- 816 [9] B. Peeters, W. Hendricx, J. Debille, Modern Solutions for Ground Vibration Testing of Large
817 Aircraft, *Sound Vib.* 295 (2009) 8–15. doi:10.4271/2008-01-2270.
- 818 [10] A. Pavic, Z. Miskovic, P. Reynolds, Modal Testing and Finite-Element Model Updating of a
819 Lively Open-Plan Composite Building Floor, *J. Struct. Eng.* 133 (2007) 550–558.
820 doi:10.1061/(ASCE)0733-9445(2007)133:4(550).
- 821 [11] D.J. Ewins, *Modal Testing: Theory, Practice and Application*, Research Studies Press Ltd.,
822 Baldock, Hertfordshire, England, 2000.
- 823 [12] A.M. Abdel-Ghaffar, R.H. Scanlan, Ambient vibration studies of Golden Gate bridge: 1.
824 Suspended structure, and 2. Pier tower structure, *ASCE J. Eng. Mech.* 111 (1985) 463–482.
825 doi:10.1061/(ASCE)0733-9399(1985)111:4(463).

- 826 [13] J.M.W. Brownjohn, E.P. Carden, C.R. Goddard, G. Oudin, Real-time performance monitoring
827 of tuned mass damper system for a 183m reinforced concrete chimney, *J. Wind Eng. Ind.*
828 *Aerodyn.* 98 (2010) 169–179. doi:10.1016/j.jweia.2009.10.013.
- 829 [14] S.K. Au, Uncertainty law in ambient modal identification---Part II: Implication and field
830 verification, *Mech. Syst. Signal Process.* 48 (2014) 34–48. doi:10.1016/j.ymsp.2013.07.017.
- 831 [15] PCB Piezotronics, PCB Piezotronics, (2017). <http://www.pcb.com/Products/model/393c>
832 (accessed October 8, 2017).
- 833 [16] Honeywell, Q-Flex QA-750, (2017).
834 [https://aerospace.honeywell.com/en/~media/aerospace/files/brochures/accelerometers/q-](https://aerospace.honeywell.com/en/~media/aerospace/files/brochures/accelerometers/q-flexqa-750accelerometer_bro.pdf)
835 [flexqa-750accelerometer_bro.pdf](https://aerospace.honeywell.com/en/~media/aerospace/files/brochures/accelerometers/q-flexqa-750accelerometer_bro.pdf) (accessed October 8, 2017).
- 836 [17] Kinematics, Episensor, (2017). https://kinematics.com/post_products/episensor-es-t/
837 (accessed October 8, 2017).
- 838 [18] L. Nachman, J. Huang, J. Shahabdeen, R. Adler, R. Kling, IMOTE2: Serious computation at the
839 edge, *Proc. IWCMC 2008 - Int. Wirel. Commun. Mob. Comput. Conf.* (2008) 1118–1123.
- 840 [19] J. a. Rice, B.F. Spencer, Jr., Structural health monitoring sensor development for the Imote2
841 platform, *Proc. SPIE - Int. Soc. Opt. Eng.* 6932 (2008) 693231–693234.
842 doi:10.1117/12.776695.
- 843 [20] M. Kane, D. Zhu, M. Hirose, X. Dong, B. Winter, M. Häckell, J.P. Lynch, Y. Wang, A. Swartz,
844 Development of an extensible dual-core wireless sensing node for cyber-physical systems, in:
845 *SPIE - Int. Soc. Opt. Eng.*, 2014: p. 90611U. doi:10.1117/12.2045325.
- 846 [21] S. Cho, H. Jo, S. Jang, J. Park, H.J. Jung, C.B. Yun, B.F. Spencer, J.W. Seo, Structural health
847 monitoring of a cable-stayed bridge using wireless smart sensor technology: data analyses,
848 *Smart Struct. Syst.* 6 (2010) 461–480.
- 849 [22] D. Zhu, Y. Wang, J.M.W. Brownjohn, Vibration testing of a steel girder bridge using cabled and
850 wireless sensors, *Front. Archit. Civ. Eng. China.* 5 (2011) 249–258. doi:10.1007/s11709-011-
851 0113-y.
- 852 [23] J. Li, T. Nagayama, K.A. Mechitov, B.F. Spencer, Efficient campaign-type structural health
853 monitoring using wireless smart sensors, in: *Proc. SPIE - Sensors Smart Struct. Technol. Civil,*
854 *Mech. Aerosp. Syst.*, 2012: p. 83450U–83450U–11. doi:10.1117/12.914860.
- 855 [24] J.M.W. Brownjohn, F. Magalhães, E. Caetano, A. Cunha, Ambient vibration re-testing and
856 operational modal analysis of the Humber Bridge, *Eng. Struct.* 32 (2010) 2003–2018.
857 doi:10.1016/j.engstruct.2010.02.034.
- 858 [25] Guralp, MAN-RTM-0003 - Real-time Clock Operator's Guide, (2016).
- 859 [26] J.M.W. Brownjohn, S.K. Au, B. Li, J. Bassitt, Optimised ambient vibration testing of long span
860 bridges, in: *EURODYN 2017, 2017*: p. 10. doi:10.1016/j.proeng.2017.09.147.
- 861 [27] Y.L. Xi, Y.C. Zhu, S.K. Au, Operational modal analysis of Brodie Tower using a Bayesian
862 approach, in: *UNCECOMP 2017 Int. Conf. Uncertain. Quantif. Comput. Sci. Eng.*, 2017: p. 10.
- 863 [28] K.Y. Wong, K.W.Y. Chan, K.L. Man, Monitoring of wind load and response for cable-supported
864 bridges in Hong Kong, in: *Proc SPIE 4337, Heal. Monit. Manag. Civ. Infrastruct. Syst.*, 2001: p.
865 12.

- 866 [29] K. Lebel, P. Boissy, M. Hamel, C. Duval, Inertial measures of motion for clinical biomechanics:
867 Comparative assessment of accuracy under controlled conditions - Effect of velocity, PLoS
868 One. (2013). doi:10.1371/journal.pone.0079945.
- 869 [30] V. Krishnamurthy, K. Fowler, E. Sazonov, The effect of time synchronization of wireless
870 sensors on the modal analysis of structures, Smart Mater. Struct. 17 (2008) 055018.
871 doi:10.1088/0964-1726/17/5/055018.
- 872 [31] J.M.W. Brownjohn, M. Bocian, D. Hester, A. Quattrone, W. Hudson, D. Moore, S. Goh, M.S.
873 Lim, Footbridge system identification using wireless inertial measurement units for force and
874 response measurements, J. Sound Vib. 384 (2016) 339–355. doi:10.1016/j.jsv.2016.08.008.
- 875 [32] R. Sleeman, Three-Channel Correlation Analysis: A New Technique to Measure Instrumental
876 Noise of Digitizers and Seismic Sensors, Bull. Seismol. Soc. Am. 96 (2006) 258–271.
877 doi:10.1785/0120050032.
- 878 [33] S.K. Au, J.M.W. Brownjohn, J.E. Mottershead, Quantifying and managing uncertainty in
879 operational modal analysis, Mech. Syst. Signal Process. 102 (2018) 139–157.
880 doi:10.1016/j.ymssp.2017.09.017.
- 881 [34] J.M. Caicedo, Practical guidelines for the natural excitation technique (NExT) and the
882 eigensystem realization algorithm (ERA) for modal identification using ambient vibration, Exp.
883 Tech. 35 (2011) 52–58. doi:10.1111/j.1747-1567.2010.00643.x.
- 884 [35] C. Gentile, N. Gallino, Ambient vibration testing and structural evaluation of an historic
885 suspension footbridge, Adv. Eng. Softw. 39 (2008) 356–366.
886 doi:10.1016/j.advengsoft.2007.01.001.
- 887 [36] K. Van Nimmen, P. Van den Broeck, P. Verbeke, C. Schauvliege, M. Malli?, L. Ney, G. De
888 Roeck, Numerical and experimental analysis of the vibration serviceability of the Bears' Cage
889 footbridge, Struct. Infrastruct. Eng. 13 (2017) 390–400. doi:10.1080/15732479.2016.1160133.
- 890 [37] S.K. Au, Operational Modal Analysis: Modeling, Bayesian Inference, Uncertainty Laws,
891 Springer, 2017.
- 892 [38] J.M.W. Brownjohn, H. Hao, T.-C. Pan, Assessment of structural condition of bridges by
893 dynamic measurements Applied Research Report RG5/97, (2001) -.
- 894 [39] P.D. Welch, The use of fast Fourier transform for the estimation of power spectra: A method
895 based on time averaging over short, modified periodograms, IEEE Trans. Audio Electroacoust.
896 15 (1967) 70–73.
- 897 [40] H. Nandan, M.P. Singh, Effects of thermal environment on structural frequencies: Part I - A
898 simulation study, Eng. Struct. 81 (2014) 480–490. doi:10.1016/j.engstruct.2014.06.046.
- 899
- 900
- 901
- 902